# JIMMA UNIVERSITY
# JIMMA INSTITUTE OF TECHNOLOGY
# FACULTY OF MECHANICAL ENGINEERING
# THERMAL SYSTEM ENGINEERING


## STUDY OF THE EFFECTS OF HEATED ETHANOL FUEL ON ENGINE PERFORMANCE AND EMISSIONS USING CFD SIMULATION

A thesis report submitted to the School of Graduate Studies of Jimma University in Partial Fulfillment of the Requirements for the Degree of Master of Science in Thermal System Engineering.


**BY:** ESHETU TADESSE

**Advisor:** BALEWGIZE AMARE (Asst. Prof.)

**Co-advisor:** DESTA GOYTOM (MSc.)



MAY 2018

JIMMA, ETHIOPIA

# DECLARATION

I, the under signed, declare that this thesis entitled by "*STUDY THE EFFECTS OF HEATED ETHANOL FUEL ON ENGINE PERFORMANCE AND EMISSIONS USING CFD SIMULATION*" is my original work, and has not been presented by any other person for an award of a degree in this or any other University, and all sources of materials used for the thesis have been duly acknowledged.

| | | |
|---|---|---|
| Eshetu Tadesse | ____________________ | ____________________ |
| Name | Signature | Date |
| Balawgize Amara (Asst. Proff.) | ____________________ | ____________________ |
| Main Advisor**:** | Signature | Date: |
| Mr. Desta Goytom | ____________________ | ____________________ |
| Co-Advisor**:** | Signature | Date |

**<u>Approved by Board of Examiners</u>**

| | | |
|---|---|---|
| Dr. Abdulkadir Aman | ____________________ | ____________________ |
| External Examiner | signature | Date |
| Mr. Nebiyou Bogale (Asst. Proff.) | ____________________ | ____________________ |
| Internal Examiner | signature | Date |
| Mr. Fikadu Kifle | ____________________ | ____________________ |
| Chair Man | signature | Date |

# ACKNOWLEDGEMENT

First and most of all, I would like to thank almighty God for blessing and being with me in every step I pass through.

I would like to express my warmest thanks my advisor Mr. Balewgize Amare and co- advisor Mr. Desta Goytom for their immense guidance and supervision all the way throughout this research work with good heart and patient.

A special thanks address to Jimma University, Institute of Technology, Faculty Mechanical engineering Staffs for their support until the completion of the study.

My special thanks goes to all my friends and my family for their support and encouragement during the development and work of the thesis.

## ABSTRACT

The use of ethanol fuel in transportation sector can contribute a better contribution on energy sustainability and mitigate environmental pollutant emissions of this sector. However, the use of ethanol fuel is still challenging, the most common use of ethanol fuel is by blending it with gasoline. In this Ethanol is mostly supplied in a splash-blended form with gasoline or in a pure form; however, this is not an optimal way of using ethanol because the use of ethanol leads to increased brake specific fuel consumption. Recently, Ethanol direct injection plus gasoline port injection (EDI+GPI) has been developed as a new technology for using ethanol fuel more effectively and efficiently in IC engine. In this study, the use of pre-heated ethanol fuel and by directly injecting the heated ethanol to the combustion chamber, and gasoline port injecting method using CFD simulation has been done, on EDI+GPI engines, to investigate the effects of heated ethanol fuel on performance and emission of engine by using ANSYS ICE package. The results show that increasing the ratio and temperature of ethanol fuel from 15% to 50% and from 300K to 340K, respectively, will enhance the performance of engine and reduce the emission from the engine. The simulation results depicted that operating the engine with ethanol fuel at a temperature of 340K produce best engine performance in terms of in-cylinder pressure and temperature for all fuel ratios. Ethanol 50% fuel ratio (i.e. ethanol 50% and gasoline 50%) gives best engine performance with additional reduction in in-cylinder temperature of the combustion chamber that significant contribution to reduce the pollutants emission of the engine.


**Key word;** Ethanol Direct Injection, Gasoline port Injection, combustion simulation, ethanol Pre-heating, engine performance, CFD simulation.

## Table of Content

**Contents** **pages**

# List of Figures

# List of Tables

# Nomenclatures

| | |
|---|---|
| $A_f$ | flame front area |
| AFR | Air Fuel Ratio |
| BDC | Bottom Dead Center |
| BSFC | break specific fuel consumption |
| $C_{1\varepsilon}$, $C_{2\varepsilon}$, $C_{3\varepsilon}$ | constants that have been determined experimentally |
| CAD | crank angle degrees |
| CAD | Computer Aided Drawings |
| CFD | computational fluid dynamics |
| CCW | counter-clock wise |
| CI | Compression Ignition |
| CO | Carbon monoxide |
| $CO_2$ | Carbon dioxide |
| $c_p$ | specific heats at constant pressure |
| Cr | Compression ratio |
| CV | Control Volumes |
| $c_v$ | specific heats at constant volume |
| CW | Clock wise |
| DI | Direct Injection |
| $d_{mi}$ | mass flow into (+) or out of (-) the cylinder |
| $D_t$ | turbulent diffusivity |
| $E$ | internal energy of the cylinder gas mixture |
| E15 | Ethanol 15% |
| E50 | Ethanol 50% |

| | |
|---|---|
| E85 | Ethanol 85% |
| EDI | ethanol direct injection |
| EVO | Exhaust Valve Opening |
| $\varepsilon$ | dissipation rate |
| FVM | Finite Volume Method |
| GDI | Gasoline direct injection |
| $G_b$ | Generation of turbulent kinetic energy that arises due to buoyancy |
| $G_k$ | Generation of turbulent kinetic energy that arises due to mean velocity gradients |
| GPI | Gasoline Port injection |
| HC | Hydrocarbon |
| $h_i$ | specific enthalpy of gas which enters or leaves the cylinder |
| $h_j^0$ | enthalpy of formation of species $j$ |
| $h_j$ | sensible enthalpy of species $j$ |
| ICE | Internal Combustion Engine |
| ICEM | Internal Combustion Engine Modeling |
| IVC | Intake Valve Closing |
| $\vec{J}_j$ | diffusion flux of species $j$ |
| k | turbulence kinetic energy |
| k-ε | K-epsilon |
| $k-\omega$ | K-Omega |
| $K_{eff}$ | effective conductivity |
| NOx | oxides of nitrogen |

| | |
|---|---|
| ODE | Ordinary Differential equation |
| $P$ | Pressure |
| PAH | Poly Aromatic Hydrocarbons |
| PDE | partial Differential equation |
| PFI | Port-Fuel-Injection |
| PI | Port injection |
| $Q$ | heat exchange of the cylinder contents with the cylinder walls |
| $\boldsymbol{q}_\phi$ | surface sources/sinks of $\phi$ |
| $\boldsymbol{r}$ | spark radius |
| RANS | Reynolds Averaging Navier-Stokes |
| $R_j$ | volumetric rate of creation of species $j$ |
| $\boldsymbol{S}$ | bounding surface |
| SI | spark ignition |
| Sox | oxides of Sulfur |
| $S_\varepsilon$ and $S_k$ | source terms defined by the user |
| $S_h$ | volumetric heat sources |
| $S_t$ | turbulent flame speed |
| $S_\phi$ | volume sources/sinks of $\phi$ |
| $T_b$ | burned gas temperature |
| Tca | Tumble ratio with the crank angle θ |
| TDC | Top Dead Center |
| TKE | Turbulent Kinetic Energy |

| | |
|---|---|
| TR | Tumble ratio |
| $T_u$ | unburned gas temperature |
| $\boldsymbol{U}$ | Fluid Velocity |
| $U_b$ | boundary velocity |
| UHC | Unburned Hydrocarbon |
| $\widetilde{u_J}$ | fluid velocity vector |
| $u_t$ | turbulent flame speed |
| V | Volume |
| $W$ | work |
| $Y_M$ | Fluctuating dilation in compressible turbulence |
| $\rho$ | density |
| $\rho_b$ | density of the burnt fluid behind of the flame |
| $\rho_u$ | density of the unburned fluid ahead of the flame front |
| $\sigma_k$ and $\sigma_\varepsilon$ | turbulent Prandtl numbers for k and $\varepsilon$, |
| $\Phi$ | tensorial property |
| $\nabla$ | tangential gradient operator |

# CHAPTER ONE

## 1. Introduction

A growing world population and industrialization has seen a commensurate increase in the demand for energy. This increase in energy demand is affecting the cost of fossil fuel and energy in the world. Transportation is among the biggest energy users in the world, where the largest share is related to engine system. This highlights the potential for considerable energy, emissions and cost savings by improving the performance of such engine systems. Over the last two decades, there has been a dramatic evolution in engine control systems which are largely driven by government regulations, customer's demand for fuel efficient vehicles and minimum safety and reliability standards that are independent of age, environment and varying fuel properties.

The internal combustion (IC) engine is today the most widely used energy source in the automotive and naval industry. It has therefore become increasingly important to improve the efficiency of the engines to reduce fuel consumption, emission levels and noise pollution to decrease the negative effect it has on the health of the human being as well as its environment. Since the introduction of the IC engine in the late 19th century its development has resulted in a constant reduction of fuel consumption and emission levels, while the power output per cylinder volume has continued to increase. The IC engine comes in many different types and sizes but can be divided in the category of the two stroke cycle or the four stroke cycle which can either be run by the Otto or the Diesel principle. For Otto engines the pre-mixed air-fuel mixture is ignited by a spark from a sparkplug. while for the Diesel principle the air is compressed beforehand in the cylinder and the incoming fuel spray is ignited by the high pressure and temperature. In this chapter a brief explanation of the four stroke, spark-ignited (SI/Otto) engine will be presented, since this is the type of engine that the work of the thesis is performed on [4].

The four stroke cycle starts with the piston positioned in TDC (Top Dead Center) and as the piston travels down towards BDC (Bottom Dead Center) the intake valve opens and the exhaust valve remain as closed, letting the fresh charge of air-fuel mixture to enter the cylinder through the intake valve during the intake stroke, see Figure 1.1(a). With the piston at BDC both the intake valve and exhaust valve closes and as the piston travels towards TDC again, the fresh charge inside the combustion chamber (cylinder) is compressed during the compression stroke, see Figure 1.1(b). As the piston reaches TDC the compressed air-fuel mixture is ignited by the spark plug and the chemical energy of the fuel is converted to heat during combustion. This increases the cylinder gas temperature and pressure therefore adding work to the crankshaft during the power stroke or expansion stroke, see Figure 1.1(c). When the piston reaches BDC again, the exhaust valve opens and as the piston travels towards TDC, the exhaust gas is pushed out from the cylinder during the exhaust stroke, see Figure 1.1(d). When the piston has reached TDC the cycle is restarted again. In one power cycle the crankshaft has done two full revolutions (720 crank angle degrees or CAD) and the piston has traveled up and down the cylinder four times, therefore the name four stroke cycle [1].

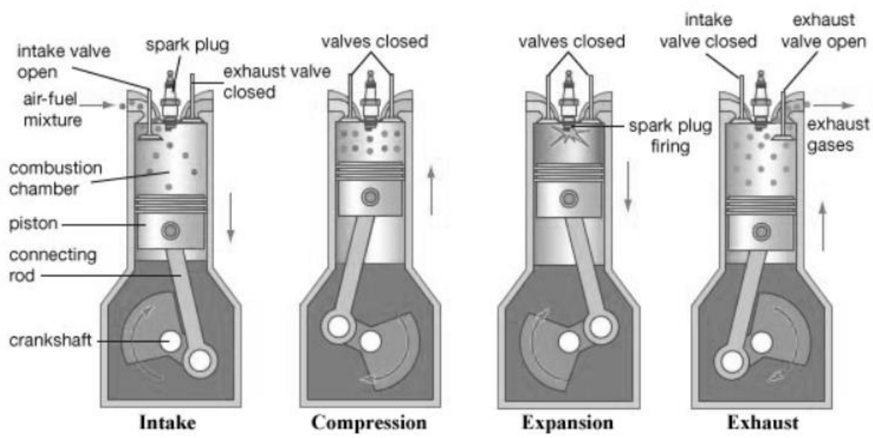


Figure 1.1. The four phases of the four stroke IC engine: (a) intake stroke, (b) compression stroke, (c) expansion or power stroke and (d) exhaust stroke [1].

## 1.1. Fuel Injection System in Spark-Ignition Engine

In SI engines the air and fuel are usually mixed together in the intake system prior to entry to the engine cylinder, using a carburetor or fuel-injection system

**Carburetor;** Venturi flow device which meters the proper amount of fuel into the air flow by means of a pressure differential. For many decades it was the basic fuel metering system on all automobile (and other) engines. It is still used on low cost small engines, but is uncommon on new automobiles[5].

Fuel injection into the intake manifold or inlet port and Fuel Direct injection to the combustion chamber is an increasingly common alternative to a carburetor in modern automobiles.

## 1.2. Direct Injection Vs. Port Injection

Right now there are two types of injection systems common on gasoline-powered vehicles these are port injection and direct injection. Both systems use computer-controlled electric injectors to spray fuel into the engine, but the difference is where they spray the fuel.
Port injection sprays the fuel into the intake ports where it mixes with the incoming air. The injectors are often mounted in the intake manifold runners and the fuel sits in the runners till the intake valve opens and the mixture is pulled into the engine cylinder.

Direct injection has the injectors mounted in the cylinder head and the injectors spray fuel directly into the engine cylinder, where it then mixes with the air. Only air passes through the intake manifold runners and past the intake valves with direct injection [6].

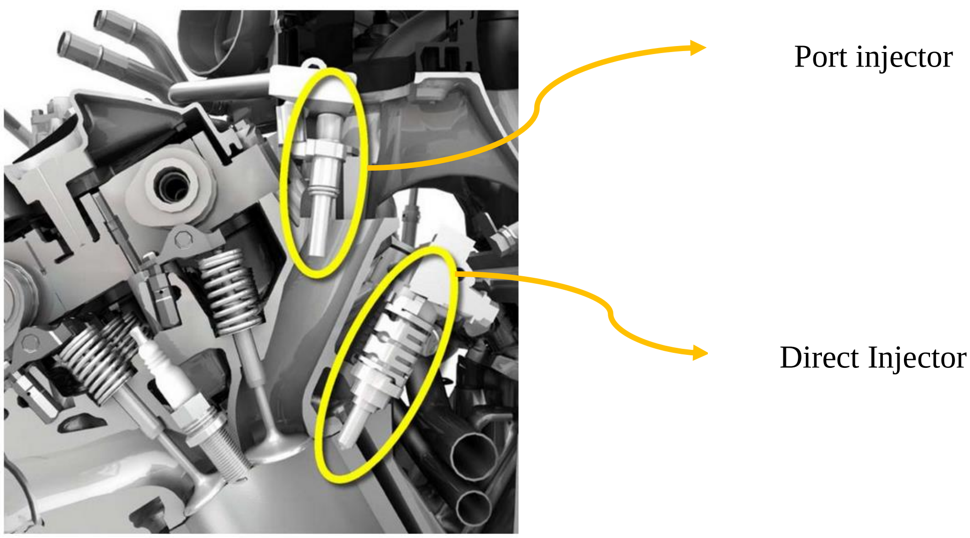


Figure 1.2 Toyota’s D-4S Lexus IS350 3.5-liter V-6 engine [4].

There are advantages and disadvantages of both systems. The biggest advantage of direct injection is its better fuel economy. Improvements of 15 percent are not uncommon just by changing from port to direct injection. Another advantage is performance. Direct injection can meter the amount of fuel exactly into each cylinder for optimum performance and it is sprayed in under very high pressure up to 15,000 PSI on some vehicles so the fuel atomizes well and ignites almost instantly.

Vaporization follows atomization. Here, the fine fuel droplets go through a liquid-to-gas phase change, becoming a vapor that can be mixed with air and ignited by the spark plug. Because heat is absorbed during this phase change, there's a cooling effect, which can be used to improve the engine's operating efficiency. With PI, the air flowing through the intake manifold is cooled before it reaches the combustion chamber. With DI, the cooling benefit occurs within the chamber itself.

PI is handy for naturally aspirated engines because cooling the incoming air increases its density and power-producing potential. It's significantly easier to locate injectors in the intake ports, well away from the valves and spark plugs. This upstream location provides ample time for full vaporization to occur.

With DI, the chance of detonation premature ignition of the fuel and air mixture is diminished because the phase-change cooling effect takes place during the compression stroke just before ignition. Lowering the combustion chamber's surface temperatures enables a higher compression ratio and improved efficiency whether the engine is naturally aspirated or boosted [4].

PFI engines commonly operate under a homogeneous-charge combustion mode and stoichiometric air fuel ratio (AFR). In addition to the homogeneous stoichiometric combustion mode, GDI engines can also run advanced combustion modes such as the stratified-charge combustion mode. In stratified-charge combustion mode, the air/fuel mixture near the spark plug is stoichiometric or slightly rich whilst in the rest of the combustion chamber it is slightly lean. The stratified-charge can be achieved by injecting all or a fraction of fuel into the cylinder during the compression stroke [7].

One downside of PI is that fuel droplets sometimes are deposited on the intake port walls, upsetting the intended fuel-air ratio.

During cold start a transient film of liquid fuel is formed in the intake valve area of the port, and some portion of it is drawn into the cylinder during each induction event. So the fuel delivered to the cylinder in each cycle differs from that metered by the injector. This causes a fuel delivery delay and an associated inherent metering error due to partial evaporation. This makes necessary to supply extra fuel for cold start, that exceeds the stoichiometric value, so that an increase of engine-out emissions of unburned hydrocarbons is experienced [8].

Disadvantages of direct injection include cost. Because the injector tips are mounted right into the combustion chamber, the materials in the injector have to be very good quality and that costs money. Also, the high pressure needed to inject fuel directly into the cylinders means that more expensive high-pressure fuel pumps are required.

The ultimate strategy is combining both PI and DI benefits, using each to diminish the other's negatives. Toyota, for example, fires both injectors during low to medium load and rpm conditions in other words, during normal driving. This raises the density of the incoming charge without boosting and flushes carbon deposits off the intake valves. During high load and rpm circumstances, when maximum combustion chamber cooling is needed because detonation is more likely, DI handles all the fuel delivery. Ford uses PI alone at idle and at low rpm for smooth, quiet, and efficient engine operation. As rpm and load increase, fuel delivery becomes a programmed blend of PI and DI. In contrast to Toyota's methodology, Ford's PI is always operating, responsible for at least 5 to 10 percent of the fuel delivery [4]. In this paper, the combined PI and DI engine type is designed for advanced engine operation and performance during hot and cold condition as well as for flexible fuel mixing purpose during engine operation.

### 1.3. Engine Design decisions

IC engine design involves several critical decisions which impact and interact with the fluid dynamics.

The primary goal of engine design is to maximize each efficiency factor, in order to extract the most power from the least amount of fuel. In terms of fluid dynamics, the volumetric and combustion efficiency are dependent on the fluid dynamics in the engine manifolds and cylinders.

The second goal of engine design is to meet emissions requirements, which are always specified by regulations. The pollutants include oxides of nitrogen (NOx), sulfur oxides (SOx), CO (carbon monoxide), unburned hydrocarbons (HC), and Poly Aromatic Hydrocarbons (PAH or "soot"), which are all products of the combustion process. Pollutants are formed by a variety of interactions of the mechanical and chemical processes inside the engine and are intimately tied to fluid dynamics in the cylinder. Though the pollutants in the exhaust stream can be reduced utilizing after-treatments, often these technologies add considerable cost to the engine. Therefore, it is desirable to minimize the pollutant formation at the source.

## 1.4. Introduction to ethanol fuel for IC engine

Ethanol also called Ethyl alcohol, is a clear, colorless liquid, with a burning taste and characteristic, agreeable odor. The chemical formula of ethanol is $C_2H_5OH$. Commercial ethanol contains 95 percent by volume of ethanol and 5 percent of water. Dehydrating agents remove the remaining water and produce absolute ethanol.

Ethanol it is extracted from the biomass and consequently has a good "well to tank" $CO_2$ emission balance. Moreover, its properties, especially in terms of octane number and latent heat of vaporization allow a large improvement of the engine.

Ethanol as a fuel for internal combustion engines is not a new concept. Indeed, the first internal combustion engines and vehicles (N. Otto in 1877, H. Ford in 1880, in 1892 in France) were drawn to run with pure alcohol (methanol or ethanol). In the United States and also in many countries such as France or United Kingdom, many studies were achieved in the 1920's and 1930's with this fuel, before the wide diffusion of leaded gasoline induced a decrease in the interest in ethanol for years. During the last decades, a renewed interest for ethanol has grown, linked with the more and more stringent emission limits. Moreover, some economical aspects, such as agricultural development (in Brazil for instance) have also favored to the use of ethanol. Finally, the Kyoto Protocol and the growing concern for greenhouse gas emissions will lead in the next coming years to an increase in biofuel productions, among which ethanol has an important role to play [9].

Ethanol is a widely used alternative fuel to address the issue of energy sustainability. Compared with gasoline fuel, ethanol has greater latent heat of vaporization, larger octane number, higher flame propagation speed and smaller stoichiometric air/fuel ratio.

The main properties of ethanol and Gasoline were summarized in Table 1.1.

Table 1.1 physical properties of Ethanol and Gasoline [7].

| | Ethanol | Gasoline(typical) |
|---|---|---|
| Molar mass (g/mol) | 46.07 | 102.5 |
| C (%wt) | 52.2 | 86.5 |
| H (%wt) | 13.1 | 13.5 |
| O (%wt) | 34.7 | 0 |
| Density ($kg/m^3$) | 794 | 735-760 |
| Latent heat of vaporization (kJ/Kg) | 854 | 289 |
| Distillation ($^oc$) | 78.4 | 30-190 |
| Net Heating Value (KJ/Kg) | 26805 | 42690 |
| Net Heating Value (kJ/I) | 21285 | 32020 |
| Stoichiometric air ratio | 8.95 | 14.4 |
| RON | 111 | 95 |
| MON | 92 | 85 |

- A very high octane number, which induces a strong resistance to knock and consequently the ability to optimize the engine (compression ratio, spark-advance) and downsizing of engines.
- The presence of oxygen in the formula, which can provide a more homogeneous fuel/air mixing and consequently a decrease in unburned or partially burned molecule emissions (HC and CO).
- The high latent heat of vaporization can induce running difficulties in cold conditions, especially cold start.
- Ethanol leads to azeotropes with light hydrocarbon fractions and can lead to volatility issues.
- Ethanol is miscible with water, which can cause demixing issues when blended with hydrocarbons.
- The high oxygen content of ethanol and its ability to oxidize into acetic acid induce compatibility issues with some materials used in the engine, such as metals or polymers.
- Ethanol combustion in engines induces aldehydes emissions, which can have a negative impact on health. These all are properties of ethanol fuel.

However, to make the use of the renewable fuels in spark ignition (SI) engines is still challenging. The most common use of Ethanol fuel is by blending it with gasoline. Doing so creates a mix that releases fewer emissions into the environment and is considered cleaner in nature. It also keeps the car in a better shape by increasing the octane rating of the fuel. Ethanol is mostly supplied in a splash-blended form with gasoline or in a pure form; however, this is not an optimal way of using ethanol because the use of ethanol leads to increased brake specific fuel consumption [10]. All in all, it is accepted by the people, governments and car companies for the many benefits it provides Recently, ethanol direct injection (EDI) has emerged as a new technology to make the use of ethanol fuel in SI engines more effectively and efficiently by taking the ethanol fuel's merits and avoiding its drawbacks [11]. Recently, ethanol direct injection (EDI) has been developed as a new technology to address the issue of knock in downsized spark ignition (SI) engines due to the strong cooling effect of EDI and ethanol's large octane number [12]. also, gasoline direct injection plus ethanol port injection (GDI + EPI) represents a more efficient and flexible way to utilize ethanol fuel in spark ignition engines. Ethanol direct injection plus gasoline port injection (EDI+GPI) is a new technology for using ethanol fuel more effectively and efficiently in IC engine [13]. Since all ethanol's have the ability to absorb water, and therefore condensation in the fuel system is absorbed and does not have the opportunity to collect and freeze. Therefore, eliminating the need and expense of adding anti-freeze product [14]. However, the current method of premixing ethanol and gasoline fuels cannot fully exploit ethanol's merits. The ethanol's lower heating value, low volatility and other properties may play a negative role to engine performance by reducing the vehicle coverage, making the engine cold start more difficult and so on. To solve the problems faced during the use ethanol fuel for engines, this thesis work introduced the use of pre-heated ethanol fuel and by directly injecting the hated ethanol fuel in to the combustion chamber, and gasoline port injecting method. The pre-heating of ethanol is done by heat recovery from exhaust gas by using heat exchangers that exchange heat released from exhaust gas.

## 1.5. Statement of the problem

Over the last few years, the emphasis on replacement for fossil fuel and reducing fuel emissions has been becoming an active research area. It is due to such a situation that the use of Ethanol-gasoline blends for IC engine has increased in recent years. Unfortunately, ethanol can cause corrosion on combustion chamber walls and piston heads of the engines when it is used as ethanol-gasoline blends. The other problem faced is that ethanol is not volatile as gasoline lading to a cold start problem in cold climates. When combustion of air/fuel mixture in the cylinder does not start correctly in response to ignition by spark plug, this directly creates engine knock.

In other countries like USA, fuel flexible vehicles are being manufactured to replace the current vehicle in addressing the problem of corrosion, utilizing large content of ethanol fuel up to 85% with gasoline 15%. However, in our country, these vehicles are not available in large quantity and only the old models are being run on ethanol-blended fuel that will lead to inefficient combustion. To address the problem of fuel combustion and emission reduction on these model vehicles further research needs to be done.

To solve this problem, this study investigates the use of pre-heated ethanol fuel by directly injecting the heated ethanol to the combustion chamber, and gasoline port injecting method. The pre-heating of ethanol has been done by method of heat recovery using a heat exchanger that recover heat released through exhaust gas.

## 1.6. Objective of the study

### 1.6.1. General objective

The main objective of this thesis is to investigate the effect of heated ethanol fuel on combustion and emissions of an Ethanol Direct Injection plus Gasoline Port Injection (EDI + GPI) engine using CFD simulation.

#### 1.6.2. Specific objective

The followings are the specific objectives of this work.

- Modelling the physical structure of standard Toyota 2NZ engine using standard dimension.
- Simulate the combustion performance of Ethanol Direct Injection plus Gasoline Port Injection by varying the percentage of ethanol from 15% to 85% and ethanol temperature from 300K to 380K.
- Design of heat exchangers and ethanol fuel pre-heating mechanism for pre-heating of ethanol.
- Validate the simulation results using experimental data from previous literature (using secondary validation method).

## 1.7. Scope of the Thesis

The scope of this work is

- Modelling and simulation of Ethanol Direct Injection plus Gasoline port injection (EDI + GPI) engine which is fueled with heated ethanol using CFD software.
- Validate the results using secondary validation method, (by using data from pervious literature).
- Design of heat exchangers and ethanol fuel pre-heating mechanism for pre-heating of ethanol fuel.
- Primary validation (experimental validation) is beyond the scope of this research.
- The engine body design and modification as well as their costs are beyond the scope of this study.

## 1.8. Significance of the Thesis

The outcome of this research can potentially lower (reduce) the dependence of IC engines on fossil fuels which means, by shifting the need for some foreign produced oil to domestically produced energy sources. This means, almost all oil consumed in Ethiopia is imported, the displacement of oil based fuels to ethanol produces a net shift from foreign to domestic energy sources.

If ethanol fuel is used for IC engines, great amount of gasoline and diesel is saved and reduce environmentally pollutant gas emission like carbon-monoxide, oxides of nitrogen and hydrocarbons. Also, the problem of knocking of engines, erosion on engine bodies, combustion problems in engines are reduced.

# CHAPTER TWO

# 2. Literature Review

## 2.1. Overview of ethanol direct and gasoline port injection engine

Namho Kim et al, in 2015; in this study, an injection system that incorporates ethanol port injection and gasoline direct injection methods was used. The effect of ethanol port fuel injection and gasoline direct injection systems on engine combustion and emission characteristics under full load conditions investigated. The experiment was conducted using two different compression ratios and various ethanol injection timings. Knock occurrence decreased as the ethanol injection timing was held while intake valves were open. Minor reductions in carbon monoxide, total hydrocarbon, and particulate emissions were observed under a compression ratio of 9.5, while the reduction in emissions became significant under a compression ratio of 13.3 as the amount of ethanol injection increased [10].

According to journal published on Energy 160 (2015), In this study, CFD modelling and experiments were carried out to investigate the charge cooling effect and combustion characteristics of ethanol direct injection in a gasoline port injection (EDI + GPI) engine. Experiments were conducted on a single-cylinder spark ignition engine equipped with EDI + GPI over a full range of ethanol ratio from 0% (GPI only) to 100% (EDI only). Simulation results showed that the overall cooling effect of EDI was enhanced with the increase of ethanol ratio from 0% to 58%, but was not enhanced with further increase of ethanol ratio. When the ethanol ratio was greater than 58%, a large number of liquid ethanol droplets were left in the combustion chamber during combustion and fuel impingement on the cylinder wall became significant, leading to local overcooling in the near-wall region and over-lean mixture at the spark plug gap. As a consequence, the CO and HC emissions increased due to incomplete combustion. Compared with GPI only, the faster flame speed of ethanol fuel contributed to the greater peak cylinder pressure of EDI + GPI condition, which resulted in higher power output and thermal efficiency [15].

In 2016**,** A full cycle numerical modelling including both port and direct injection sprays was performed for Ethanol direct injection plus gasoline port injection (EDI + GPI) engine to understand the mechanisms behind the experimental results of the EDI + GPI engine. The performance of engines fueled with neat ethanol fuel was investigated. The results showed the advantages of using pure ethanol fuel in the tested conditions. However, as neat fuel, ethanol may be not suitable to power SI engines in some conditions because of its low volatility, low heating value and high enthalpy of vaporization, especially under cold conditions [16].

According to research held in 2016, paper reports the investigation of the effect of EDI heating on the combustion and emissions of a research engine equipped with EDI + GPI. The results showed that EDI heating effectively reduced the CO and HC emissions of the engine due to the increase of evaporation rate and reduced fuel impingement and local over-cooling. The reduction of CO and HC became more significant with the increase of ethanol ratio [17].

According to the study held in 2016 by Y. Huang, the spray and evaporation characteristics of ethanol and gasoline fuels injected from a multi-hole injector were investigated by high speed Shadowgraphy imaging technique in a constant volume chamber. Results showed that ethanol and gasoline sprays demonstrated the same patterns in non-evaporating conditions. The sprays could be considered as non-evaporating when vapor pressure was lower than 30 KPa. Ethanol evaporated more slowly than gasoline did in low temperature environment, but they reached the similar evaporation rates when temperature was higher than 375 K. This suggested that EDI should only be applied in high temperature engine environment [18].

In 2015 a research done by B. Harshavardhan at el, a CFD analysis using a commercial software has been carried out with different combustion chamber shapes formed by using different piston top profiles in a two-valve four-stroke engine. From the analysis, it is observed that, combustion chamber shape with pent roof-offset-bowl piston gives about 221.5% higher tumble ratio and about 59.5% higher turbulent kinetic energy of in-cylinder flows, and about 6.8% higher percentage of fuel evaporation as compared to those of dome piston. Therefore, combustion chamber shape with pent-roof offset-bowl piston is better suited as compared to other combustion chamber shapes [19].

## 2.2. SPARK PLUG

Starting characteristics, service life, performance, fuel consumption, and exhaust performance, all these critical engine parameters are influenced by the spark plug. The ignition system on petrol-driven engines in contrast to diesel engines is external: at the end of compression stroke, an electrical spark produced by the spark plug triggers the combustion of the compressed fuel-air mixture. It is the task of the spark plug to generate this spark. Created by the high voltage produced by the ignition coil, it leaps between the electrodes. A flame front spreads from the spark and fills the combustion chamber until the mixture has been burned. The heat released increases the temperature, there is a rapid buildup of pressure in the cylinder and the piston is forced downwards (Power stroke). The movement is transferred via the connecting rod to the crankshaft; this drives the vehicle via the clutch, the gears and the axles.

In order for the engine to operate smoothly, powerfully and in an environmentally friendly manner, a number of requirements have to be met, the correct amount of perfectly balanced fuel/ air mixture must be present in the cylinder, and the high-energy ignition spark must leap between the electrodes precisely at the predetermined moment. For this purpose, spark plugs have to meet the highest performance requirements: they must deliver a powerful ignition spark between around 500 and 3,500 times a minute (in 4-stroke operation) - even during hours of driving at high revs or in stop-and-go traffic conditions. Even at -20 °C, they have to ensure a completely reliable ignition. High-tech spark plugs provide low-emission combustion and optimum fuel efficiency without misfiring [20].

### 2.2.1. A modern spark plug must meet the following requirements

1. **Electrical requirements**
    - Reliable high-voltage transmission, even at ignition voltages of up to 40,000 volts
    - Good insulation capability, even at temperatures of 1,000 °C, prevention of arcing and flashover
2. **Thermal requirements**
    - Resistance to thermal shock (hot exhaust gases – cold intake mixture)
    - Good thermal conduction by insulator tip and electrodes
3. **Mechanical requirements**
    - Pressure-tight and gas-tight sealing of the combustion chamber, resistance to oscillating pressures up to approx. 100 bar
    - High mechanical strength for reliable installation
4. **Electrochemical requirements**
    - Resistance to spark erosion, combustion gases and residues
    - Prevention of build-up of deposits on the insulator

### 2.2.2. Spark plug design and types

**A. Materials**

The electrodes in spark plug typically consist of high-nickel alloys, while the insulators are generally made of aluminum oxide ceramic and the shell is made of steel wire. Material used for spark plug must offer good thermal conductivity and high corrosion resistance for long operating lives and to fulfill critical engine parameters.

**B. Electrode gap**

The shortest distance between the central and earth electrode(s) on the spark plug has been called the electrode gap. This is what the ignition spark must jump across. The optimum electrode gap in any particular situation depends partly on the engine, and it is determined in close collaboration with the vehicle manufacturer. Maximum precision in maintaining the electrode gap is important since an incorrect gap can have a considerable detrimental effect on spark plug function and consequently on engine performance

- If the electrode gap is too small this may cause misfiring, noisy idling and poor exhaust gas quality levels.
- If the electrode gap is too large, this may lead to misfiring.
- The coordinated spark positioning on multi-electrode plugs means the electrode gaps does not have to be adjusted

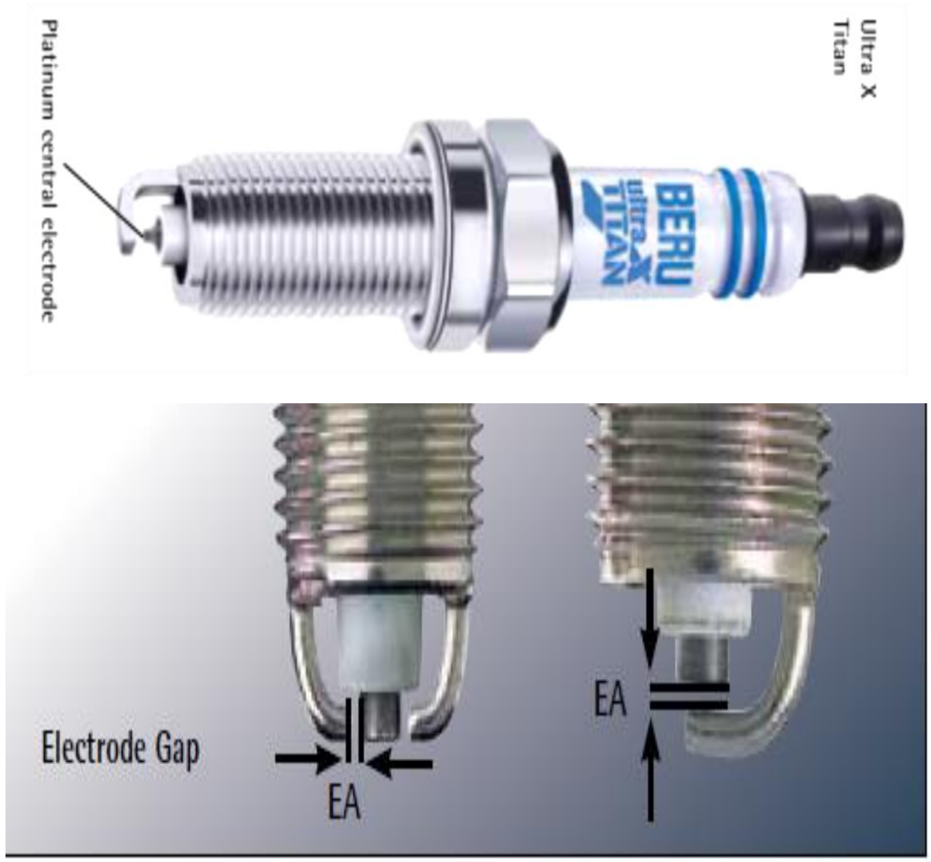


Figure 2.1 Spark plug and electrode gap of BERU spark plug [18].

### C. Spark position and Spark distance

The function of the spark plug in the combustion chamber is influenced by three main factors: the spark position, the spark distance and the electrode gap for spark plugs using variable spark technology. Spark position is the name given by engine developers to the spark path geometry, the extent to which the spark path extends into the combustion chamber.

## D. Thermal rating

The thermal rating is a measure of the thermal structure of a spark plug. It indicates the maximum thermal loading on the spark plug in equilibrium between heat absorption and heat dissipation.

It is vital to choose the correct thermal rating when selecting a spark plug:

- ✓ If the thermal rating characteristic is too high (for example thermal rating 9) the plug is unable to dissipate the resultant heat quickly enough. This leads to incandescent ignition; in other words, it is not the ignition spark that ignites the mixture but the overheated plug.

- ✓ If the thermal rating characteristic is too low (for example thermal rating 5) then the free burning temperature required in the lower performance range for self-cleaning the plug, is not reached. Result: misfiring, increased fuel consumption and higher exhaust emissions.

  BERU spark plugs are highly specialized, precision components, which have been developed to meet vehicle manufacturers' specifications and are produced on up to date production lines. Therefore, since this BERU spark plug are manufactured with advanced technology, this thesis paper selected the BERU spark plug for entire design.

## 2.3. Gasoline Direct Injection Fuel Injector

The main purpose of direct fuel injection system is to deliver fuel into the cylinder of the engine. The major advantages of a GDI engine are increased fuel efficiency and high power output. Emissions levels can also be more accurately controlled with the GDI system. The cited gains are achieved by the precise control over the amount of fuel and injection timings that are varied according to engine load. In order for the engine to effectively make the use of this fuel.

I. Fuel must be injected in proper time, that is, the injection timing must be controlled

II. The correct amount of fuel must be delivered to meet power requirement, that is, injection metering must be controlled.

However, it is still not enough to deliver an accurately metered amount of fuel at the proper time to achieve good combustion. Additional aspects are critical to ensure proper fuel injection system performance including:

- **Fuel atomization;** ensuring that fuel atomizes into very small fuel particles is a primary design objective for diesel fuel injection systems. Small droplets ensure that all the fuel has a chance to vaporize and participate in the combustion process.

- **Bulk mixing;** While fuel atomization and complete evaporation of fuel is critical, ensuring that the evaporated fuel has sufficient oxygen during the combustion process is equally as important to ensure high combustion efficiency and optimum engine performance.

- **Air utilization;** Effective utilization of the air in the combustion chamber is closely tied to bulk mixing and can be accomplished through a combination of fuel penetration into the dense air that is compressed in the cylinder and dividing the total injected fuel into a number of jets [21].

The direct injector that used for this thesis paper with the above requirement is Delphi Multec® GDI Multi-Hole Fuel Injectors.

Delphi Multec GDI Multi-Hole Fuel Injectors can be applied to any size gasoline engine, from small displacement turbocharged engines to large displacement engines, including central mount applications. It offers flexible spray preparation options that allow customization of the spray shape to accommodate a wide variety of combustion chamber shapes [3]. The performance specification of Delphi multec injector is listed in table below.

Table **2.1** Delphi multec injector and Targeted Performance Specifications [3].

| | Multec 12 Injector | Multec 12.1 Injector |
|---|---|---|
| Static flow rate | Up to 20 g/sec | Up to 20 g/sec |
| Closing response time | 0.4 msec | 0.4 msec |
| Opening response time | 0.4 msec | 0.4 msec |
| Fuel pressure | 30 to 260 bar | 30 to 300 bar |
| Qmin flow at 100 bar, 7.2 g/sec static flow, 3 sigma | 5.0 mg/pulse | 3.5 mg/pulse (no compensation) |
| $D_{32}$ sauter mean diameter (SMD) | 7 μm (at 200 bar) | 6 μm (at 300 bar) |
| $DV_{90}$ | 16 μm (at 200 bar) | 14 μm (at 300 bar) |
| 0 after inject (no bounce) | No bounce at close | No bounce at close |
| Cone angle as required by combustion | 40° to 90° | 40° to 90° |

## 2.4. The role of CFD simulation on engine design

IC engines involve complex fluid dynamic interactions between air flow, fuel injection, moving geometries, and combustion. Fluid dynamics phenomena like jet formation, wall impingement with swirl and tumble, and turbulence production are critical for high efficiency engine performance and meeting emissions criteria. The design problems that are encountered include port-flow design, combustion chamber shape design, variable valve timing, injection and ignition timing, and design for low or idle speeds.

There are several tools which are used in practice during the design process. These include experimental investigation using test or flow bench setups, 1D codes, analytical models, empirical/historical data, and finally, computational fluid dynamics (CFD). Of these, CFD has the potential for providing detailed and useful information and insights that can be fed back into the design process.

CFD simulations can be a powerful engineering tool that can help to understand the thermo-physical and chemical processes that takes place in an IC engine without being forced to use possibly complicated and expensive measurement techniques. Some things (such as the flow or temperature field in the cylinder) can be difficult to measure in a three dimensional space and one dimensional models does not account for all geometric topologies, making CFD simulations an important compliment. It can also be a valuable tool to run numerous tests and investigations of an engine without having to perform them in a test bench which can reduce development costs. CFD simulations can also serve as a fast and cheap way to perform studies of future engine designs and concepts before a prototype is manufactured, reducing development costs further. This is because in CFD analysis, the fundamental equations that describe fluid flow are being solved directly on a mesh that describes the 3D geometry, with sub-models for turbulence, fuel injection, chemistry, and combustion. Several techniques and sub-models are used for modeling moving geometry motion and its effect on fluid flow.

Using CFD results, the flow phenomena can be visualized on 3D geometry and analyzed numerically, providing tremendous insight into the complex interactions that occur inside the engine. This allows to compare different designs and quantify the trade-offs such as soot Vs NOx, swirl vs. tumble and impact on turbulence production, combustion efficiency Vs pollutant formation, which helps determine optimal designs. Hence CFD analysis is used extensively as part of the design process in automotive engineering, power generation, and transportation. With the rise of modern and inexpensive computing power and 3D CAD systems, it has become much easier for analysts to perform CFD analysis.

CFD research has unfortunately not yet reached a state where it completely describes all the processes that takes place in an IC engine. This is mainly due to the fact that it is a highly complex mechanical device which incorporates many, simultaneously interacting, thermo fluid and chemical processes. Because of the IC engines reciprocating nature it features extreme deformation of the solution domain due to the moving piston and valves, and the shape of the piston and cylinder head, which are key features for the engine design, are usually very complex. Aside from the geometric complexity there are also the simultaneously interacting thermo fluid processes such as; non-stationary turbulent flow, heat and mass transfer, injection, atomization, dispersion and vaporization of the liquid fuel, ignition, combustion and the consequent formation of harmful pollutants, to mention a few. Adding all this together makes a complete modeling of the IC engine one of the most challenging task in the area of CFD research [4].

## 2.5. Heat Exchanger Design for EDI heating

A heat exchanger is a device that is used to transfer thermal energy (enthalpy) between two or more fluids, between a solid surface and a fluid, or between solid particulates and a fluid, at different temperatures and in thermal contact. Typical applications involve heating or cooling of a fluid stream of concern and evaporation or condensation of single or multicomponent fluid streams. In other applications, the objective may be to recover or reject heat, or sterilize, pasteurize, fractionate, distill, concentrate, crystallize, or control a process fluid [22].

### 2.5.1. HEAT EXCHANGER SELECTION AND DESIGN CONSIDERATIONS

**Problem Specifications.** The first and most important consideration is to select the design basis (i.e., design conditions). Next comes an analysis of the performance at the design point and off-design (turndown) conditions. The design basis would require the specification of operating conditions and the environment in which the heat exchanger is going to be operated. These include fluid mass flow rates (including fluid types and their thermo-physical properties), inlet temperatures and pressures of both fluid streams, required heat duty and maximum allowed pressure drops on both fluid sides, fluctuations in inlet temperatures and pressures due to variations in the process or environment parameters, corrosiveness and fouling characteristics of the fluids, and the operating environment (from safety, corrosion/erosion, temperature level, and environmental impact points of view). In addition, information may be provided on overall size, weight, and other design constraints, including cost, materials to be used, and alternative heat exchanger types and flow arrangements

**Exchanger Specifications**. Based on the problem specifications and the design engineer's experience, the exchanger construction type and flow arrangement are first selected. Selection of the construction type depends on the fluids (gas, liquid, or condensing/evaporating) used on each side of a two-fluid exchanger, operating pressures, temperatures, fouling and cleanability, fluids and material compatibility, corrosiveness of the fluids, how much leakage is permissible from one fluid to the other fluid, available heat exchanger manufacturing technology, and cost. The choice of a particular flow arrangement is dependent on the required exchanger effectiveness, exchanger construction type, upstream and downstream ducting, packaging envelope/ footprint, allowable thermal stresses, and other criteria and design constraints. The orientation of the heat exchanger, the locations of the inlet and outlet pipes, and so on, dictated by the system and/or available packaging/footprint space and ducting [23].

To select an appropriate heat exchanger, the researcher would firstly consider the design limitations for each heat exchanger type. Also, the weight and size of heat exchangers used in transportation or vehicle applications are very important parameters, and in these cases cost considerations are frequently subordinated insofar as material and heat-exchanger construction costs are concerned; however, the weight and size are important cost factors in the overall application in these fields and thus may still be considered as economic variables.

There are three main types of heat exchangers:

a) The Recuperative type in which the flowing fluids exchanging heat are on either side of a dividing wall.
b) The Regenerative type in which the hot and cold fluids pass alternately through a space containing a matrix of material that provides alternately a sink and a source for heat flow.
c) The Evaporative type in which a liquid is cooled evaporatively and continuously in the same space as the coolant.

This research paper is on recuperative type of heat exchanger, which can further be classified, based on the relative directions of the flow of the hot and cold fluids, into three types:

By using the above heat exchangers selection and design considerations and specifications, in this research paper the recuperative double-pipe heat exchanger type of heat exchanger were selected for preheating of ethanol fuel. The double-pipe heat exchanger is one of the simplest, cheapest for both design and maintenance, making them a good choice for this research paper. It is called a double-pipe exchanger because one fluid flows inside a pipe and the other fluid flows between that pipe and another pipe that surrounds the first. This is a concentric tube construction. Flow in a double-pipe heat exchanger can be co-current (parallel flow) or counter-current (counter flow) as shown figure 2.2. In co-current flow (parallel flow), both the hot and cold fluids enter the heat exchanger at the same end and move in the same direction**.** In counter current (counter flow), the hot and cold fluids enter the heat exchanger at opposite ends and flow in opposite directions. This type of flow arrangement allows the largest change in temperature of both fluids and is therefore most efficient (where efficiency is the amount of actual heat transferred compared with the theoretical maximum amount of heat that can be transferred) [1]**.**

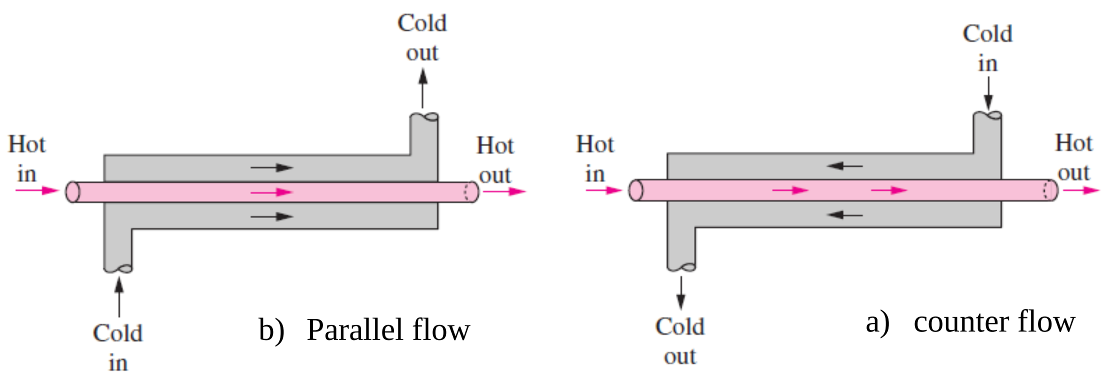


Figure 2.2 flow regimes of double-pipe heat exchanger [1].

In this research paper the double-pipe heat exchanger used for preheating of ethanol fuel is located on exhaust manifold of the engine, which exchanges heat with exhaust gas released from the combustion chamber. Which recover thermal heat flux from exhaust gas of the engine, by accomplishing with the specific pressure drops limits on both exhaust gas and working fluid side.

# CHAPTER THREE

## 3. Mathematical Models used for CFD simulation in ICE

The main concept of CFD is the discretized solution of a set of partial differential equations commonly known as the Navier-Stokes equations. These equations are discretized in time, by solving the equations in small time steps, and in space by dividing the domain in a large number of small computational cells or control volumes (CV). The space discretized solution domain is commonly referred to as the computational grid or mesh. The method commonly used for space discretization is called the Finite Volume Method (FVM), and for a static mesh (no moving boundaries) it is based on the integral form of the conservation equation over a control volume, CV, fixed in space. But simulating the fluid dynamics in a combustion engine requires moving boundaries of the solution domain, since the structure of the flow field is very much dependent on the moving piston and valves. When the mesh has moving boundaries the integral form of the conservation equation for a tensorial property $\phi$ defined per unit mass in an arbitrary moving volume V bounded by a closed surface $S$ [2].

$$\frac{d}{dt}\int_{V}^{\cdot}\rho\emptyset dV+\oint_{S}^{\cdot}dS\cdot\rho\emptyset(U-U_{b})=-\oint_{S}^{\prime}dS\cdot\rho q_{\emptyset}+\int_{V}^{\prime}S_{\emptyset}dV \quad \ldots\ldots\ldots\ldots\ldots\ldots (3.1)$$

where $\rho$ is the density, $U$ is the fluid velocity, $U_b$ is the boundary velocity, $q_{\phi}$ and $S_{\phi}$ are the surface and volume sources/sinks of $\phi$ respectively. Since the volume V is no longer fixed in space, its motion is captured by the motion of its bounding surface $\boldsymbol{S}$ by the velocity $U_b$.

### 3.1. Internal Combustion Engines in ANSYS Workbench

ANSYS Workbench provides an ideal integrated environment for engines with powerful tools for geometry, meshing, CFD solvers, and post-processing available on a common platform.

In ANSYS Workbench,

- Bidirectional CAD connectivity ensures that design changes from CAD are automatically propagated into the simulation.
- The geometry tool (Design Modeler) can be linked to the meshing tool (ANSYS Meshing or Forte Sector Mesh Generator).

- ANSYS Meshing in turn can be linked to ANSYS Fluent or Forte and Forte Sector Mesh Generator is linked to Forte.
- The results can be automatically sent to CFD-Post, a post-processing tool.
- The data generated at each stage is stored in an organized structure and can be easily exchanged between different tools.

All of these tools can be linked together in "systems" in ANSYS Workbench and provide a built-in pathway for simulation automation. In addition, each tool has built-in technological capabilities for creating process compression tools to automate repeated tasks, such as geometry decomposition and cleanup, meshing, solution setup and solver runs; and post-processing. Thus ANSYS Workbench has tremendous potential as a platform for process compression and solution automation [24]**.**

In increasing order of complexity, the CFD analyses of IC engines performed on ANSYS workbench can be classified into [25]**.**

- ❖ **Port Flow Analysis**: Quantification of flow rate, swirl and tumble, with static engine geometry at different locations during the engine cycle.
- ❖ **Cold Flow Analysis**: Engine cycle with moving geometry, air flow, and no fuel injection or reactions.
- ❖ **In-Cylinder Combustion Simulation**: Power and exhaust strokes with fuel injection, ignition, reactions, and pollutant prediction on moving geometry.
- ❖ **Full Cycle Simulation**: Simulation of the entire engine cycle with air flow, fuel injection, combustion, and reactions.

### 3.1.1. In-Cylinder Combustion Simulation

Since this paper focus on engines combustion simulation let introduce about ANSYS combustion simulation. Combustion simulation involves simulation of the power stroke during the engine cycle, starting from closing of valves to the end of the power stroke. Since the valves are closed or in the process of closing, the combustion chamber is the chief flow domain, and the piston the sole moving part.

Typically, the initial flow field at this stage is obtained from

- ✓ a cold flow simulation if the full geometry is used
- ✓ patching-in based on a cold flow analysis
- ✓ running the piston without combustion to obtain charge compression

Models are used to account for the fuel spray, combustion and pollutant formation. For direct injection engines, the fuel spray from the tip of the nozzle injector is introduced at the specific crank angle and duration using a spray model. A chemical mechanism describing the reaction of vapor fuel with air is used to describe combustion, and models for turbulence-chemistry interaction are specified. Sub-models for NOx and soot formation are used to calculate pollutant formation, which can be coupled with the combustion calculation or calculated as a post-processing step.

### 1. *The Energy model;*

ANSYS Fluent allows you to include heat transfer within the fluid and/or solid regions in any simulation model. Problems ranging from thermal mixing within a fluid to conduction in composite solids can therefore be handled by ANSYS Fluent. When ANSYS Fluent model includes heat transfer, the relevant physical models for heat transfer must enabled and the thermal boundary conditions should have supplied, and material properties that govern heat transfer and/or vary with temperature as part of the setup should be entered. Then ANSYS Fluent solves the energy transfer by using equation below [2].

$$\frac{\partial}{\partial t}(\rho E) + \nabla \cdot \left(\vec{V}(\rho E + P)\right) = \nabla \cdot \left(K_{eff}\nabla T - \sum h_j \vec{J}_j + \left(\bar{\bar{\tau}}_{eff} \cdot \vec{V}\right)\right) + S_h \qquad \text{............ (3.2)}$$

Where

- $K_{eff}$ is the effective conductivity ($k + k_t$ , where $k_t$ is the turbulent thermal conductivity, defined according to the turbulence model being used)
- $\vec{J}_j$ is the diffusion flux of species $j$
- $S_h$volumetric heat sources, the source of energy due to chemical reaction $S_{h,rxn} = \sum_j \frac{h_j^0}{M_j} R_j$
- $h_j^0$ is the enthalpy of formation of species and $R_j$ is the volumetric rate of creation of species $j$
- $E = h - \frac{p}{\rho} + \frac{v^2}{2}$

- $h_j$ sensible enthalpy of species $j$ which is defined as $h_j = \int_{T_{ref}}^{T} C_{p,j} dT$
- $\rho$ density

The first three terms on the right-hand side of equation 3.2 represent energy transfer due to conduction, species diffusion, and viscous dissipation, respectively.

### 2. Turbulence Modeling

Turbulence is the three-dimensional unsteady random motion observed in fluids at moderate to high Reynolds numbers. Turbulence can be defined as the random motion of fluid particles in the fluid flow, but vortex generation in the combustion chamber is the rotational movement of air will be helpful in providing proper mixing of air and fuel than the other turbulence motion. The exception to this are those flows in the corners and small crevices of the combustion chamber, where the close proximity of the walls dampens out the turbulence. As technical flows are typically based on fluids of low viscosity, almost all technical flows are turbulent. Another important characteristic of turbulence is that it is not a property of fluid but fluid flow. Many quantities of technical interest depend on turbulence, including:

- Mixing of momentum, energy and species
- Heat transfer
- Pressure losses and efficiency
- Forces on aerodynamic bodies

Because of the inherently chaotic characteristic of turbulence, there is no unique or general model which approximates the essence of physics of turbulence. Indeed, it is seen that in order to find the Reynolds stresses by using Navier-Stokes equations one needs to solve infinite number of equations for infinite number of variables. The main target of turbulence modeling is to model the Reynolds stresses. Many models have been developed with many specific assumptions related to the problem.

RANS (Reynolds Averaging Navier-Stokes) models offer the most economic approach for computing complex turbulent industrial flows. Typical examples of such models are the $k - \varepsilon$ or $k - \omega$, the models in their different forms. These models simplify the problem to the solution of two additional transport equations and introduce an Eddy-Viscosity (turbulent viscosity) to compute the Reynolds Stresses. RANS models are suitable for many engineering applications and typically provide the level of accuracy required.

### 3. Standard k-ε Model

K-epsilon (k-ε) turbulence model is the most common model used in computational fluid dynamics (CFD) to simulate mean flow characteristics for turbulent flow conditions. It is a two-equation model which gives a general description of turbulence by means of two transport equations (PDEs). The standard $K - \varepsilon$ model in ANSYS Fluent falls within this class of models and has become the workhorse of practical engineering flow calculations in the time. Robustness, economy, and reasonable accuracy for a wide range of turbulent flows explain its popularity in industrial flow and heat transfer simulations. It is a semi-empirical model, and the derivation of the model equations relies on phenomenological considerations and empiricism [2].

The standard k-ε model is a model based on model transport equations for the turbulence kinetic energy (k) and its dissipation rate ($\varepsilon$). The model transport equation for (k) is derived from the exact equation, while the model transport equation for (ε) was obtained using physical reasoning and bears little resemblance to its mathematically exact counterpart. The turbulence kinetic energy,$k$, and its rate of dissipation, $\varepsilon$ , are obtained from the following transport equations [2]:

$$\frac{\partial}{\partial t}(\rho k) + \frac{\partial}{\partial x_i}(\rho k u_i) = \frac{\partial}{\partial x_j}\left[\left(\mu + \frac{\mu_t}{\sigma_k}\right)\frac{\partial k}{\partial x_j}\right] + G_k + G_b - \rho\varepsilon - Y_M + S_k \ldots\ldots\ldots\ldots (3.3)$$

$$\frac{\partial}{\partial t}(\rho\varepsilon) + \frac{\partial}{\partial x_i}(\rho\varepsilon u_i) = \frac{\partial y}{\partial x_j}\left[\left(\mu + \frac{\mu_t}{\sigma_\varepsilon}\right)\frac{\partial \varepsilon}{\partial x_j}\right] + C_{1\varepsilon}\frac{\varepsilon}{k}(G_k + C_{3\varepsilon}G_b) - C_{2\varepsilon}\rho\frac{\varepsilon^2}{k} + S_\varepsilon \ldots\ldots (3.4)$$

where $G_k$ represents the generation of turbulent kinetic energy that arises due to mean velocity gradients, $G_b$ is the generation of turbulent kinetic energy that arises due to buoyancy, and $Y_M$ represents the fluctuating dilation in compressible turbulence that contributes to the overall dissipation rate. $S_\varepsilon$ and $S_k$ are source terms defined by the user. $C_{1\varepsilon}$, $C_{2\varepsilon}$ and $C_{3\varepsilon}$ are constants that have been determined experimentally. $\sigma_k$ and $\sigma_\varepsilon$ are the turbulent Prandtl numbers for k and $\varepsilon$, respectively.

### 4. Standard K-Omega Turbulence Model

FLUENT uses a standard K-Omega model developed by Wilcox (1998) that was formulated to better compute Low-Reynolds number effects, compressibility, and shear flow spreading. The standard model is an empirical based model with transport equations for turbulent kinetic energy ($k$) and its specific dissipation rate ($\omega$). This model has been modified numerous times in an attempt to improve its accuracy and as a result the transport equations used in Fluent. One of the weak points of the Wilcox model is the sensitivity of the solutions to values for $k$ and $\omega$ outside the shear layer (freestream sensitivity).While the new formulation implemented in ANSYS Fluent has reduced this dependency, it can still have a significant effect on the solution, especially for free shear flows. Due to this the $k - \omega$ model not commonly used by ICE solvers for engine simulation.

### 5. Near-Wall Treatments for Wall-Bounded Turbulent Flows

Turbulent flows are significantly affected by the presence of walls. Near walls, where the turbulent Reynolds number is low, very close to the wall, viscous damping reduces the tangential velocity fluctuations, while kinematic blocking reduces the normal fluctuations. Obviously, the mean velocity field is affected through the no-slip condition that has to be satisfied at the wall. Numerous experiments have shown that the near-wall region can be largely subdivided into three layers. In the innermost layer, called the “viscous sublayer”, the flow is almost laminar, and the (molecular) viscosity plays a dominant role in momentum and heat or mass transfer. In the outer layer, called the fully-turbulent layer, turbulence plays a major role. Finally, there is an interim region between the viscous sublayer and the fully turbulent layer where the effects of molecular viscosity and turbulence are equally important as shown. Figure 3.1 illustrates these subdivisions of the near-wall region, plotted in semi-log coordinates [2].

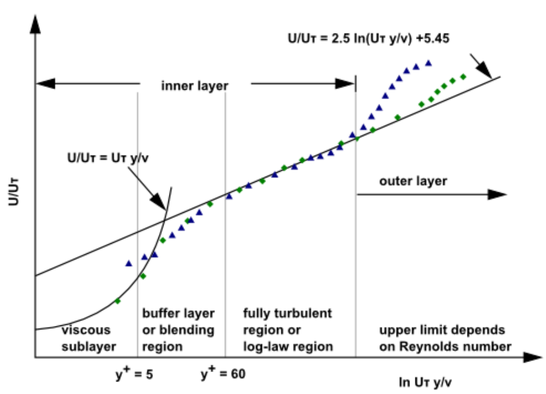


Figure 3.1 Subdivisions of the Near-Wall Region [2].

The turbulence not isotropic, and the dissipation rate must be modified accordingly. Wall functions are a set of semi-empirical formulas and functions that in effect “bridge” or “link” the solution variables at the near-wall cells and the corresponding quantities on the wall. A number wall function approaches have been used to generalize the model for wall-bounded flows. These are Standard Wall Functions, Scalable Wall Functions, Non-Equilibrium Wall Functions, User-Defined Wall Functions. The standard wall functions work reasonably well for a broad range of wall-bounded flows.

Standard wall function method is to take advantage of the fact that (for equilibrium turbulent boundary layers), a log-law correlation can supply the required wall boundary conditions. Therefore, standard wall functions have been most widely used in industrial flows, and they are provided as a default option in ANSYS Fluent.

## 3.2. Modelling of Combustion stroke

The basic equation for the engine model that is derived from first law of thermodynamics is:

$$dE = -\delta Q - \delta W + \sum_i h_i d_{mi} \quad (3.5)$$

Where

- $E$ – the internal energy of the cylinder gas mixture
- $Q$ – the heat exchange of the cylinder contents with the cylinder walls
- $W -$ the work
- $h_i -$ the specific enthalpy of gas which enters or leaves the cylinder,
- $d_{mi} -$ is the mass flow into (+) or out of (-) the cylinder
- $\delta W -$ can be expressed as *P.dV*, where *P* is the pressure and *V* is the cylinder volume

During combustion stroke, using conservation of mass and energy and the state equations, the rate of cylinder pressure *P*, unburned and burned gas temperature $T_u$ and $T_b$ are calculated as [26].

For cylinder pressure

$$\frac{dp}{d\theta} = \left(\frac{C_{v,u}}{C_{p,u}} - \frac{C_{v,b}}{R_b}\frac{R_u}{C_{v,u}} V_u + \frac{C_{v,b}}{R_b} V\right)^{-1} - \left(1 + \frac{C_{v,b}}{R_b}\right) P \frac{dV}{d\theta} - C_{p,b} T_b \times \frac{dm_{l,b}}{d\theta} - \frac{R_u}{R_b} C_{p,b} T_u \frac{dm_{i,u}}{d\theta} - \left[(e_b - e_u) - C_{v,b}\left(T_b - \frac{R_u}{R_b} T_u\right)\right]\frac{dm_b}{d\theta} + \left(\frac{C_{v,u}}{C_{p,u}} - \frac{C_{v,b}}{R_b}\frac{R_u}{C_{p,u}}\right)\frac{dQ_u}{d\theta} - \frac{dQ}{d\theta} \quad (3.6)$$

where subscripts $u$ and $b$ denote unburned and burned properties, respectively, and subscript l, denotes leakage (due to blow by). Also, $c_v$ and $c_p$ are the specific heats at constant volume and pressure, respectively, e is the specific energy and $\frac{dm_{l,b}}{d\theta}$ is the mass burning rate

unburned gas temperature [26].

$$\frac{dT_u}{d\theta} = \frac{1}{m_u C_{p,u}} \left( Vu \quad \frac{dp}{d\theta} - \frac{dQ_u}{d\theta} \right) \quad \ldots\ldots (3.7)$$

Burned gas temperature

$$\frac{dT_b}{d\theta} = \frac{p}{m_b R_b}\left[\frac{dv}{d\theta} - \left(\frac{V_b}{m_b} - \frac{V_u}{m_u}\right)\frac{dm_b}{d\theta} + \frac{V_b}{m_b}\frac{d_{m,b}}{d\theta} + \frac{V_u}{m_u}\frac{dm_{ml,b}}{d\theta} + \left(\frac{V}{P} - \frac{R_u}{C_{p,u}}\frac{V_u}{P}\right)\frac{dp}{d\theta} + \frac{R_u}{C_{p,u}\,P}\frac{dQ_u}{d\theta}\right] \quad \ldots\ldots (3.8)$$

mass burning rate:

$$\frac{dm_b}{d\theta} = \rho_v A_f u_t \quad \ldots\ldots (3.9)$$

where $\rho$ is the density, $A_f$ is the flame front area and $u_t$ is the turbulent flame speed.

## 3.3. Spark Model Theory

Typically, the initial spark size is small relative to the cell size, and the spark is under-resolved on the CFD mesh. Modeling the spark by burning a few cells around the spark location shows strong sensitivity to the grid and time-step size, and flame speed and flame brush diffusion can be erroneous due to the insufficient space and time resolution. In addition, for cases where the initial spark is smaller than the cell size, ignition proceeds too quickly. To mitigate this sensitivity, ANSYS Fluent solves a sub-grid equation for the spark evolution. The spark shape is assumed to be perfectly spherical, with an infinitely thin flame front. The spark radius,$r$, grows in time,$t$, according to the ODE [2],

$$\frac{\boldsymbol{dr}}{\boldsymbol{dt}} = \frac{\boldsymbol{\rho_u}}{\boldsymbol{\rho_b}} S_t \quad \ldots\ldots (3.10)$$

Where;

- $\rho_u$ is the density of the unburned fluid ahead of the flame front?
- $\rho_b$ is the density of the burnt fluid behind of the flame, and
- $S_t$ is the turbulent flame speed

The flame speed is modeled using G-Equation model. A *G*-equation-based combustion model incorporating detailed chemical kinetics for Spark-Ignition (SI) engine simulations for better predictions of flame propagation and pollutant formation. A progress variable concept is introduced into the turbulent flame speed correlation to account for the laminar to turbulent evolution of the spark kernel flame. This *G*-equation-based flamelet combustion model incorporating detailed chemical kinetics for both Port-Fuel-Injection (PFI) and Direct-Injection (DI) Spark- Ignition (SI) engine combustion simulations [27]**.** The G equation model is based on the flamelet modeling assumptions and uses a level-set method to describe the evolution of the flame front as an interface between the unburned and burned gases.[28]. The averaged G-equation is given as [28].

$$\bar{\rho}\frac{\partial(\overline{G})}{\partial t} + \bar{\rho}\,\widetilde{u_J}\frac{\partial \bar{G}}{\partial x_j} = \bar{\rho}D_t|\nabla\bar{G}|\nabla\left(\frac{\nabla\bar{G}}{|\nabla\bar{G}|}\right) + \bar{\rho}S_t|\nabla\bar{G}| \qquad \ldots\ldots\ldots\ldots\ldots\ldots\ldots\ldots\ldots (3.11)$$

Where

- G is a scalar field defined such that the flame front position is at G = G0, and that G is negative in the unburned mixture.
- $S_t$ The turbulent flame speed
- The term $\bar{\rho}S_t|\nabla\bar{G}|$ represents the reaction rate $(\widetilde{\dot{\omega}})$
- $\widetilde{u_J}$ the fluid velocity vector
- $D_t$ is the turbulent diffusivity
- $\nabla$ is the tangential gradient operator

# CHAPTER FOUR

# 4. ENGINE MODELING

In this stage, the both physical and mathematical model of Toyota 2NZ engine is modeled by using ANSYS ICE solver in workbench. IC Engine (Internal Combustion Engines in Workbench) is a customized application to setup and solve the flow and combustion inside an IC engine. IC Engine system is used for quantification of flow rate, swirl and tumble, and other flow parameters and combustion of air-fuel mixture inside the engine during the engine cycle with moving geometry.

## 4.1. Geometry modeling

The engine geometry used for the simulations carried out in this thesis was constructed by ANSYS DesignModeler. The ANSYS DesignModeler application is a parametric feature-based solid modeler designed in ANSYS workbench, so that we can intuitively and quickly begin drawing 2D sketches, modeling 3D parts, or uploading 3D CAD models for engineering analysis preprocessing, also to be used as a geometry editor of existing CAD models.

The CAD model is done for engine called 2NZ Engine which is used for Toyota vehicles. The basic 2NZ engine has four cylinders with a total displacement of 1000 cc with four valves per cylinder. It has port injection and a centrally located spark plug in the pent roof type cylinder head. The detailed of engine data is presented in table 4.1

Table 4.1. Engine specification data

| | measurement |
|---|---|
| Bore | 75 mm |
| Stroke | 84.7 mm |
| Crank radius | 55 mm |
| Connecting rod length | 155 mm |
| IVC | 570 CA |
| EVO | 833 CA |
| Compression ratio | 10.1 |
| Speed (rpm) | 2000 |

A multi-hole injector with an injection pressure of 40 bar is mounted along the engine axis on the cylinder head is modelled. The EDI injector was installed near to the intake manifold in between spark plug and intake manifold, with the spray plumes bent towards the spark plug in the EDI + GPI engine to create an ignitable mixture around the spark plug by the time of ignition and for clearance of exhaust gas from combustion chamber during exhaust stroke. The dimension and specification of Direct Injector used for this paper is taken from the dimension and specification of Delphi Multec GDI Multi-Hole Fuel Injectors, since in this work, Delphi Multec GDI Multi-Hole Fuel Injectors are used.

Table 4.2. The Delphi Multec GDI Multi-Hole Fuel Injectors parameters.

| | |
|---|---|
| No of holes | 6 |
| Fuel | Ethanol |
| Fuel injection timing | 575 CA |
| Injection duration | 21.5 degree |
| Injection pressure | 40 bar |
| Spray cone angle | $9^o$ |

Spark plug is design at the top center ($0^o$ from the cylinder axis) of the engine head, the dimensions and specifications used for BERU spark are presented in table 4.3.

Table 4.3. Dimensions and specification of spark plug.

| | measurement |
|---|---|
| type | I series IK22 |
| Electrode gap | 0.7 mm |
| duration | 0.003 s |
| energy | 0.2J |
| Flame speed model | Turbulent length |
| Start crank angle | $718^o$ |

In the original CAD model the elevation and plan view of the engine fluid domain geometry shown in Figure 4.1, the two intake valves and the two exhaust valves are visible as well as the intake duct (left) and exhaust duct (right). Both exhaust valves and intake valves are canted 28 $^o$c from the cylinder axis and normal to the surfaces of the combustion chamber. Here, the analysis is done compression and combustion strokes, that means from 570° (Intake Valve Closing) to 833° (Exhaust Valve Opening) CAD (crank angle degree) by considering symmetry at mid-plane of the EDI + GPI engine to reduce the complexity of the geometry and to speed up the simulation time during the entire simulation.

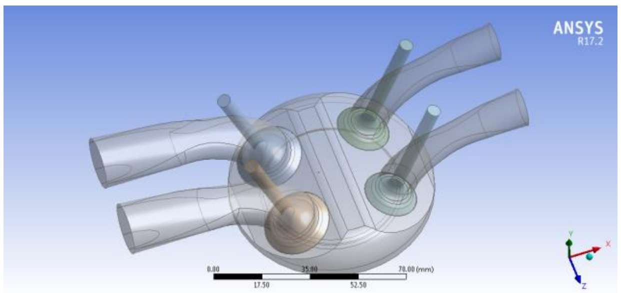


a) 3D model of the full engine

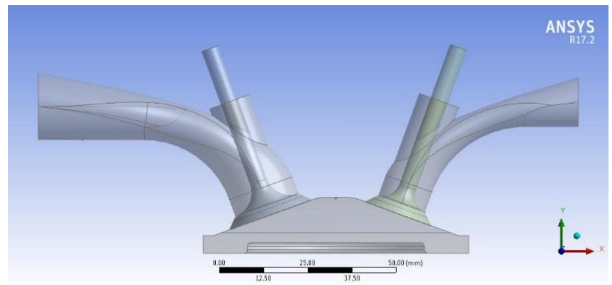


b) Front view of symmetry engine with one intake and exhaust valve.

Figure 4.1 The full and symmetry 3D model of the engine fluid domain geometry

After modelling the geometry of fluid domain for combustion chamber. the model should be prepared for decomposition. The geometry preparation for decomposition can be done by input manager located in the IC Engine toolbar. The Input Manager dialog allows us to specify input parameters related to DesignModeller at first step, with minimum possible information. This information is used to perform automatic decomposition and animation of engine motion in DesignModeller. The general input manager process for Full Engine IVC to EVO combustion simulation option and the decomposed geometry was presented in fig 4.2.

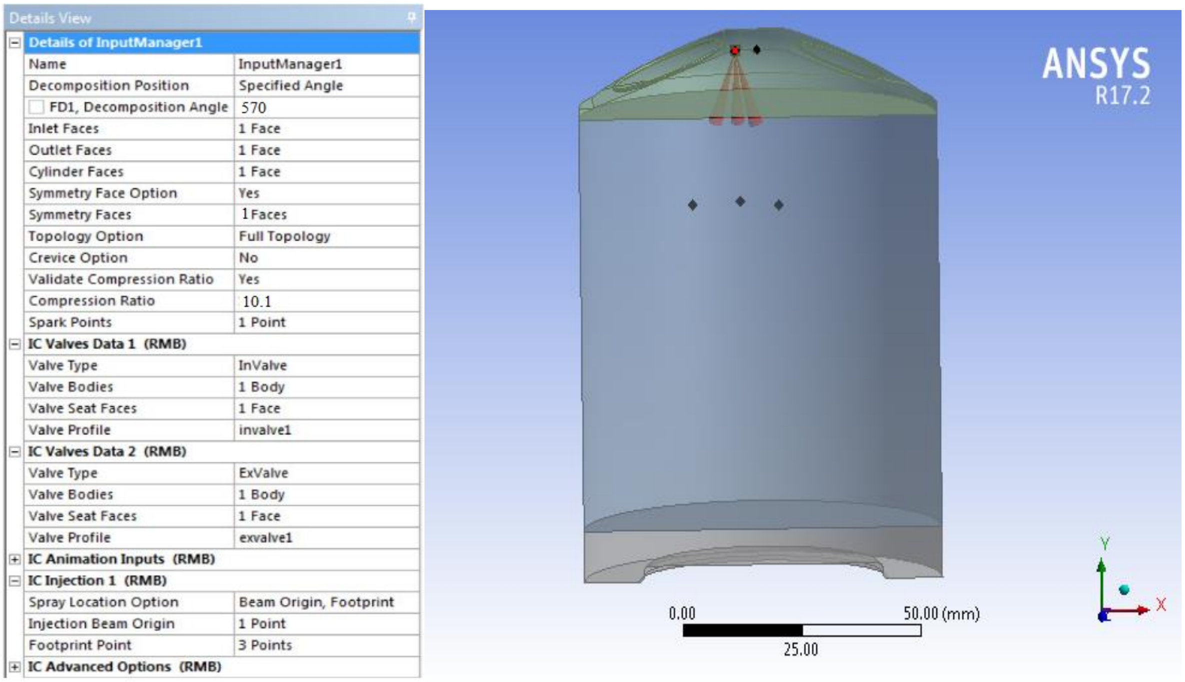


a) The general input manager settings

b) decomposed geometry with decomposition angle at IVC (570$^{o}$)

Figure 4.2 The general input manager process for Full Engine IVC to EVO combustion simulation option and the decomposed geometry

## 4.2. Meshing in IC Engine

Mesh generation is a combination of CAD model generation as well as CAD clean-up and termed as pre-processing in the entire CFD simulation process. Pre-processing means, before we move ahead to the solver we need to process CAD model in order to fit into the solver or provide the solver with the correct information.

Mesh or grid is defined as a discrete cell or elements into which the domain/ model is divided. All the flow variables & any other variables are solved at centers of these discrete cells. This entire process of breaking up a physical domain into smaller sub-domains (elements/ cells) is called as mesh generation. It is the initial step in doing analysis of any geometry. It is done in ICEM CFD software of ANSYS. After doing the meshing, analysis is done in ANSYS Workbench.

The decomposed geometry is used to generate the mesh. The goal of the IC Engine meshing tool is to minimize the effort required to generate a mesh for the IC Engine specific solver. It uses the named selection created in the decomposition to identify different zones and creates the required mesh controls. Once the meshing cell opened, meshing process for Full Engine IVC to EVO combustion simulation is done by clicking the IC Setup Mesh located in the IC Engine toolbar. Here different mesh setting for the different parts and virtual topologies defined. The mesh type used for this simulation is course mesh to minimize the time taken during the simulation process and to save computer memory, since increasing mesh size reduces the number of elements as shown in figure 4.3.

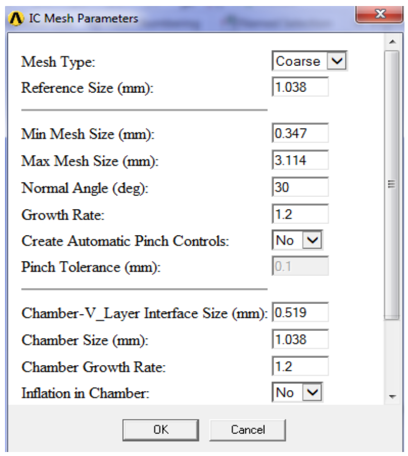


Figure 4.3 ANSYS ICE Mesh Parameters

After setting the all mesh parameters, mesh will be generated by the ANSYS meshing tool. The mash result is presented in figures below.

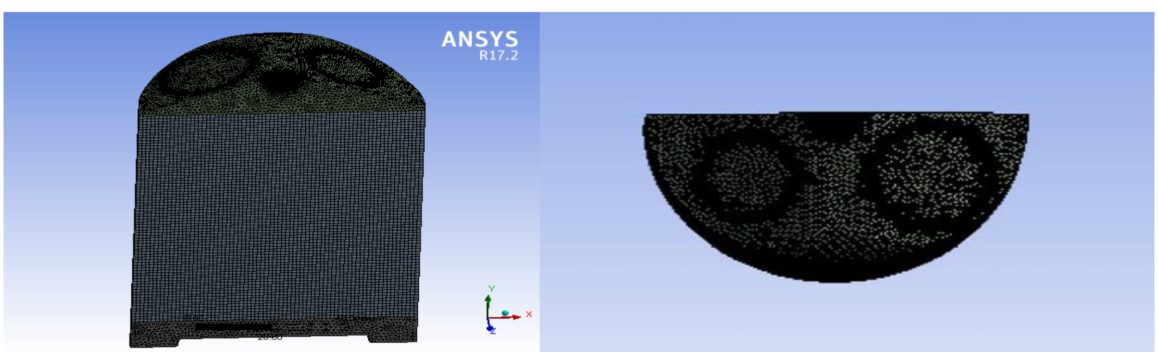


Figure 4.4 The 3D front and top view of mesh result on mesh cell.

**Mesh Report**

**Table 2.** Mesh Information for ICE

| Domain | Nodes | Elements |
|---|---|---|
| fluid ch | 44673 | 240539 |
| fluid layer cylinder | 122946 | 230092 |
| fluid piston | 23072 | 120919 |
| All Domains | 190691 | 591550 |

Figure 4.5 Report of mesh count and node count of the cell zones of ICE

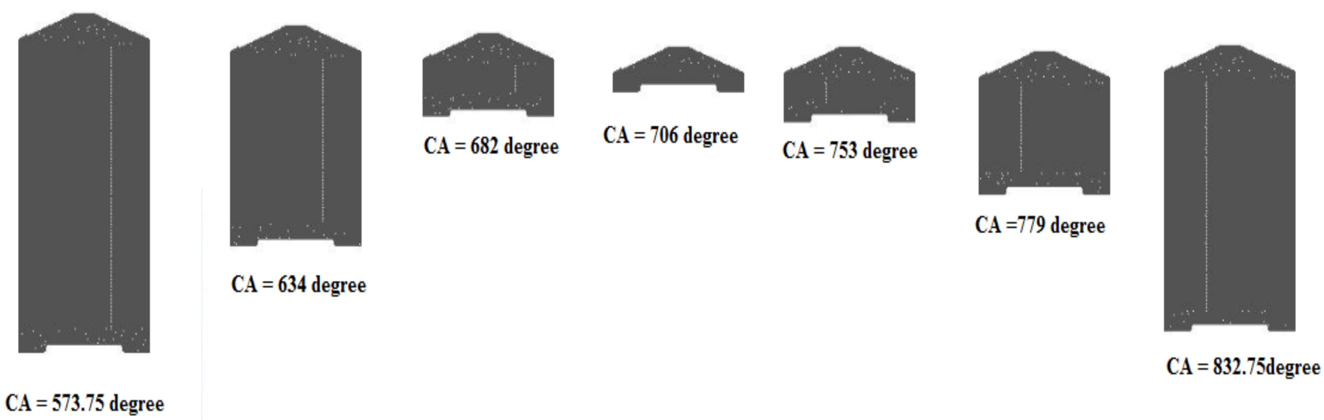


Figure 4.6 mesh result at different crank angle

## 4.3. ICE Solver Setup for Combustion Simulation

After meshing the boundary conditions and solver parameters are set as per the decomposition crank angle set in the input manager. In this stage there are seven settings to be set for combustion simulation of IC engines in ANSYS workbench, this can be done in solver setting dialog box as shown in fig 4.7, these are basic setting, physics settings, boundary conditions, monitor definitions, initialization, solution control and post-processing.

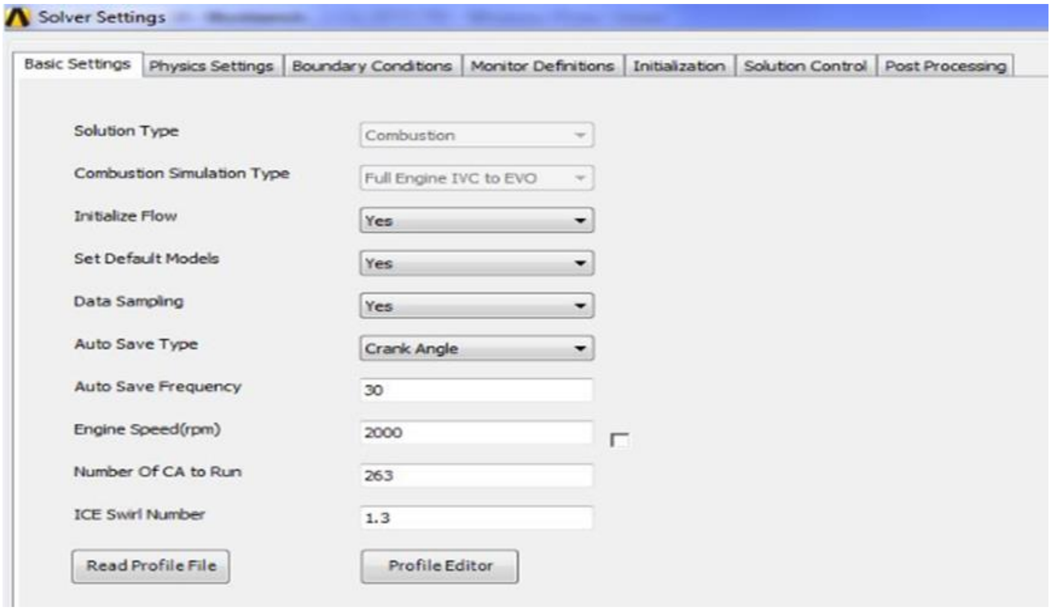


Figure 4.7**;** ANSYS ICE Solver Settings dialog box

The detail of each main solver setting is presented in the following topics.

### 4.3.1. Basic Settings

In the Basic Settings tab, the solution type and combustion simulation type used is shown (which selected in the Properties view of the ICE cell). In this the engine speed, number of crank angle to run is sated, the engine speed used for this simulation is 2000 rpm and result auto save frequency is 30$^{o}$. Since the simulation is interested only in the compression and power stroke (i.e. from IVC and EVO), the value IVC and EVO entered as 570 and 833. So the Number of CA to Run is automatically calculated from these values, therefore the number of CA to run is set to 263. In the read profile option, the mass flow rate and velocity profile of direct injector with variable crank angle is imported. This the injector profiles are extracted from port flow and cold flow simulation.

### 4.3.2. Physics Settings

In physics settings the type of engine to be simulated is selected (i.e. either CI or SI engine) for this paper simulation, the type of engine selected SI engine and partially pre-mixed model is selected for species model, since partially pre-mixed model is present only for SI Engine. ANSYS Fluent provides a partially premixed combustion model that is based on the non-premixed combustion model and the premixed combustion model.

In chemistry tab under chemkin file and Thermal Data File, the chemkin file and a thermodynamic data file of mixture properties is imported from ANSYS forte chemkin that is suitable for this simulation. Because ANSYS forte employs a fuel library file to obtain liquid thermo-physical properties and the thermodynamics and transport data for fuel vapor species employed in simulation. G-Equation is selected in the Premixed Model and peters model is used for Flame Speed Model.

In the injector tab the material, distribution diameter, temperature, Start CA (the crank angle at which the injection will start), End CA (the crank angle at which the injection will stop), injector flow rate and velocity magnitude of injector and location of injector on engine body is located by using rectangular coordinate system. The start of injection for this simulation is $575^{o}$ by using [10] as reference for the start of the Direct injection of gasoline injections. The total injection properties of injector for single simulation is shown in figure 4.8.

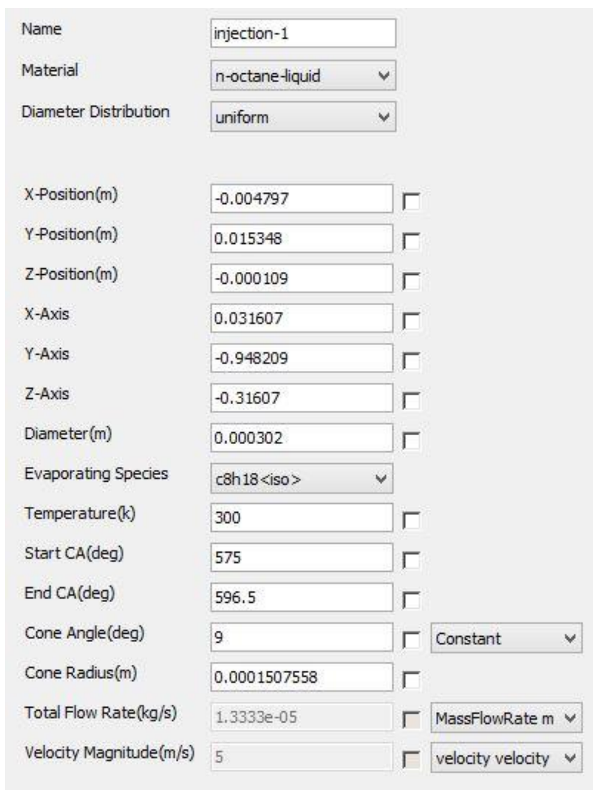


Figure 4.8; fluent injection properties dialog box for injector 0

In spark tab in physics setting tab the spark properties would be sated, in this the start crank angle of spark is entered as per simulation requirement.

### 4.3.3. Boundary Conditions

In this section, the boundary conditions applied in this study are explained. In IC combustion simulation, the most encountered boundaries are the wall and far-field inlet. In this section the Cell zone and boundary conditions provided to specify the flow and thermal variables on the boundaries of physical model. The wall boundary condition used for this paper and their thermal properties for one simulation is shown in figure 4.9

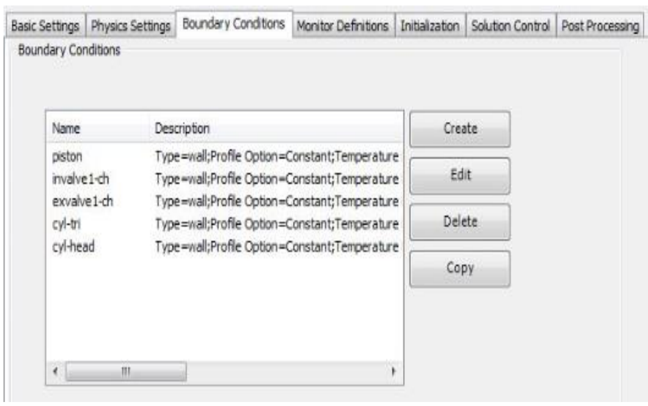


**Table 4.** Boundary Conditions

| Type | Zones | Values |
|---|---|---|
| wall | cyl-piston | Temperature (k) 500 |
| wall | cyl-quad | Temperature (k) 500 |
| wall | invalve1-ch | Temperature (k) 485 |
| wall | exvalve1-ch | Temperature (k) 485 |
| wall | cyl-tri | Temperature (k) 500 |
| wall | cyl-head | Temperature (k) 485 |
| wall | piston | Temperature (k) 485 |

Figure 4.9; wall boundary condition and their thermal properties

### 4.3.4. Monitor Definitions

In the Monitor Definitions tab, several monitors have been set on the zones ice-fluid-chamber-bottom, ice-fluid-chamber-top, and ice-fluid-piston. These monitors used to check the output results of the parameters. some monitors for used in this paper are; -

- max-pres-mon plots the Max Pressure.
- max-temp-mon plots the Max Temperature.
- vol-avg-pres-mon plots the Volume Integral of Pressure
- mass-avg-tke-mon plots the Mass Average of Turbulent Kinetic Energy.

### 4.3.5. Post-processing

The post processing setting is used to set how the result should be saved in their respective solutions. In this the result should be saved in the form of image and table at different crank angle and cut plane. In figure 4.10, shows an example of one of the images created to save temperature magnitude in ice-cutplane_1. In this images are saved from the Start Crank Angle of 570 (IVC) to the End Crank Angle of 833 (EVO) at a Frequency of every 4 time-steps. Around ten images were created in each simulation to capture the result of different parameters (like temperature, velocity, pressure, TKE, CO emission, etc.)

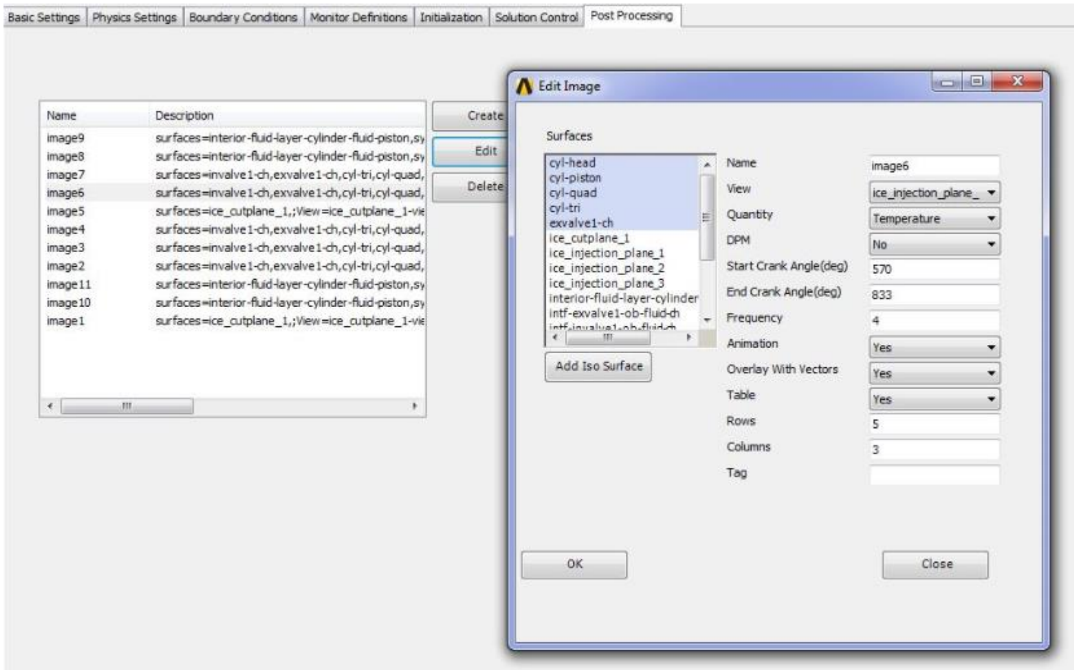


Figure 4.10; image created to capture temperature on cut_plane_1

## 4.4. Settings ANSYS ICE Solver

When ANSYS ICE setup cell opened, FLUENT Launcher opens by reading the mesh file and sets up the IC Engine case. This ANSYS FLUENT Launcher will;

- Read the valve and piston profile.
- Create various dynamic mesh zones.
- Create interfaces required for dynamic mesh setup.
- Set up the dynamic mesh parameters.
- Set up the required models.
- Set up the default boundary conditions and material.
- Create all the required events.
- Sets up the under-relaxations factors.
- Set up the default monitors.
- Initialize and patch the solution.

In the ANSYS Fluent application, we can check the default settings and edit settings for our simulation by highlighting the items in the navigation pane. This setting can be done by editing the main default setting of ANSYS ICE that are exist in the navigation pane, these settings are the setup, the solution and the result settings. In this the following setups which is shown in fig.4.11 should be done as per simulation requirement.

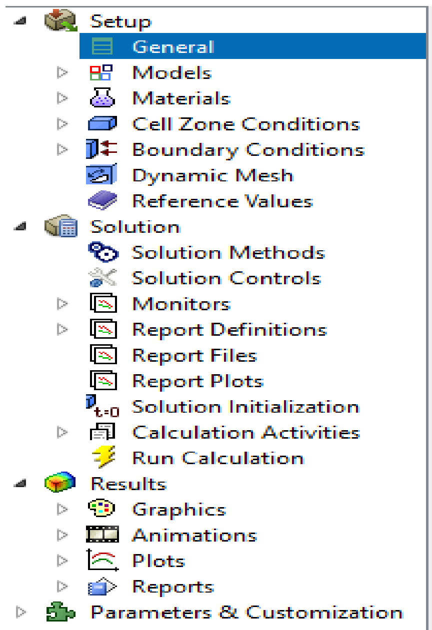


Figure 4.11. ANSYS Fluent Navigation Pane

### 4.4.1. general setting

In the general setting the Solver Type is set to Pressure-Based due the flow of fluid inside the engine occur due to the pressure difference between the engine manifold and the injector with combustion chamber, this pressure difference leads the flow of fluid from high pressure to lower one. Since the simulation is time dependent Solver Time is set to Transient and velocity formulation is set to absolute.

### 4.4.2. Models

The models used for analysis combustion simulation of IC engine are;

**I. The Energy model;**

ANSYS Fluent allows to include heat transfer within the fluid and/or solid regions in any simulation model. Problems ranging from thermal mixing within a fluid to conduction in composite solids can therefore be handled by ANSYS Fluent. To allow the heat transfer analysis in the energy model is enabled in fluent solver navigation pane under energy tab.

**II. Viscous models**

The viscous models used to set the turbulence model used for simulation of ICE combustion simulation.

From viscos models, the Standard k-epsilon model is selected, with Standard Wall Functions as Near-Wall Treatment is selected. See section 3.1.1. for the details of turbulence model, standard K-epsilon model and for selection criteria.

**III. Species model**

Depending upon selection in the Solver Settings dialog box options the partially pre-mixed combustion model, with G-equation as pre-mixed model is selected from the list of models under Species. See section 3.1.1. for detail about partially pre-mixed combustion model and G-equation model. In the boundary tab under species model dialog box the species boundary of fuel species and air filled as per percentage used in the simulation. Also, in species the spark ignition and NOx model enabled, since the simulation is done on spark ignition engine. For the rest models solver default selection retained. Then the materials used for this combustion simulation is created and or edited in materials tab. However, in this simulation the materials are imported from ANSYS chemkin data in IC solver setting stage, therefore no need of materials addition in this stage.in this the properties of n-heptane fluid materials should be edited for injection materials this is because in the injector setup, the material setup available is n-heptane therefore the properties of this material is represented by ethanol property. After finishing all setups for the simulation the solution is started. The solution calculation takes a longer time with minimum of five days and above per one simulation.

## 4.5. Model validation

In order to validate the developed model, several literatures were reviewed and the results of the combustion model are compared with the available experimental data from literatures. The selected test case is an experimental configuration which is well described in literature and it is presented in [26]. The validation is done during the compression and power stroke of the engine with the same case as literatures and the result observed from the simulation and the data presented in the literatures are presented in figure 4.12. The engine set-up specification and mixture composition was collected from literature [26].

A diagrams for in-cylinder pressure (Pa) versus crank shaft position (crank angle) were verified with data from [26]. As shown in figure 4.12, the computed values correctly follow the previous experimental data from literatures for the given engine speeds and operating conditions.it is observed from figure 4.12 that the graph of in-cylinder pressure of the simulation result is smother and wider than the experimental results. In all the cases, the simulation results reasonably well agreement achieved with the experiments during the compression and expansion stroke. Finally, in this paper it concluded that the model presented was useful in predicting flow and combustion of air and fuel in IC engines.

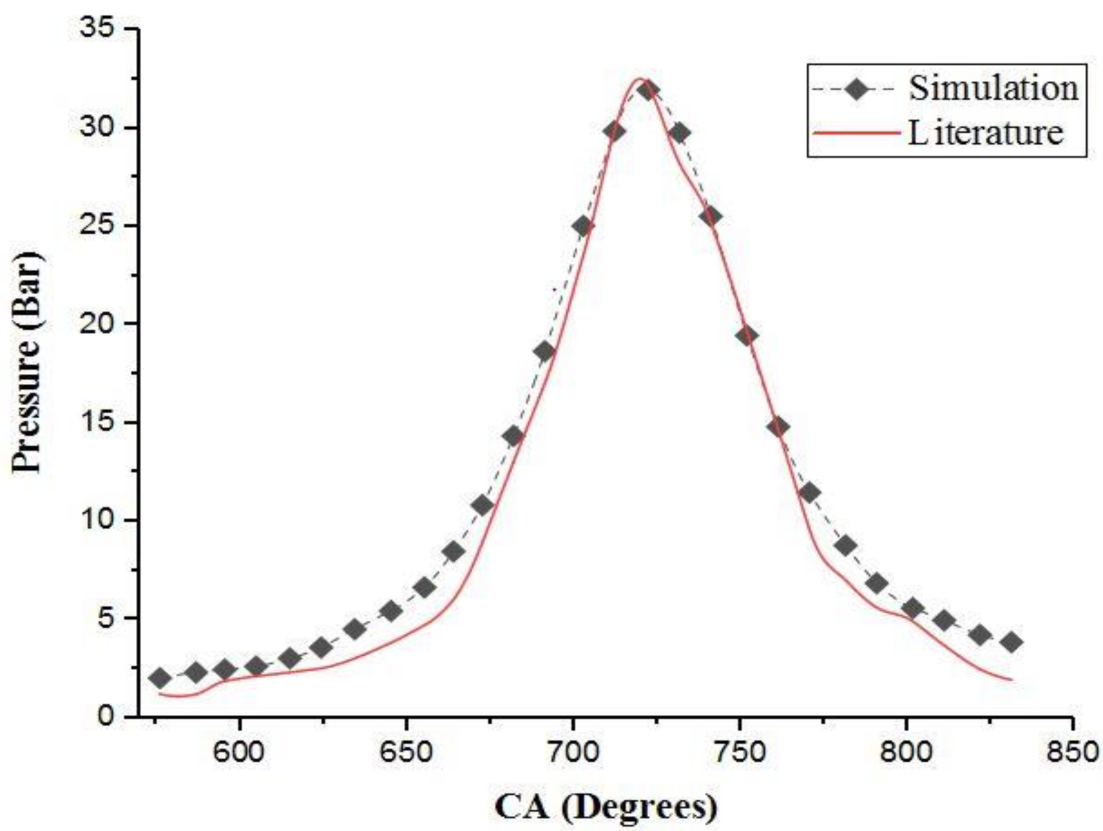


Figure 4.12. In-cylinder pressure versus crank angle position comparison between previous experimental and simulated data.

# CHAPTER FIVE

# 5. Result and discussion

The engine was tested in EDI + GPI conditions to investigate the effect of ethanol content and Ethanol temperature on the engine performance and engine emission. The engine speed constant about 2000rpm for all conditions. In this paper, a numerical investigation was used to get better insight into the in-cylinder details. SI engine performance and emission characteristics are directly affected by the type of fuel. These characteristics can be evaluated on the basis of its in-cylinder pressure, in-cylinder temperature, turbulent kinetic energy, tumble ratio and swirl ratio. The details of these characteristics can be presented and discussed one by one as follows.

## 5.1. Turbulence

Due to the high velocities involved, all flows into, out of, and within engine cylinders are turbulent flows. As a result of turbulence, thermodynamic transfer rates within an engine are increased by an order of magnitude. Heat transfer, evaporation, mixing, and combustion rates all increase. As engine speed increases, flow rates increase, with a corresponding increase in swirl, squish, and turbulence. This increases the real-time rate of fuel evaporation, mixing of the fuel vapor and air, and combustion. Turbulence in a cylinder is high during intake, but then decreases as the flow rate slows near BDC. It increases again during compression as swirl, squish, and tumble increase near TDC. Swirl makes turbulence more homogeneous throughout the cylinder. The high turbulence near TDC when ignition occurs is very desirable for combustion. It breaks up and spreads the flame front many times faster than that of a laminar flame. The air-fuel is consumed in a very short time, and self-ignition and knock are avoided. Local flame speed depends on the turbulence immediately in front of the flame. This Turbulence in IC engines is mainly due to Swirl ratio and Tumble ratios created inside the combustion chamber, details of these parameters have been presented in section below.

### 5.1.1. Swirl ratio

Swirl greatly enhances the mixing of air and fuel to give a homogeneous mixture in the very short time available for this in modern high-speed engines. It is also a main mechanism for very rapid spreading of the flame front during the combustion process.

It is a dimensionless parameter to quantity the rotational motion within the cylinder. It can also be the ratio of angular speed to the engine speed or the ratio of swirl tangential speed to the average piston speed. Figure 5.1 shows how swirl ratio changes through a cycle of the engine. During intake it is high, decreasing after BDC in the compression stroke due to viscous drag with the cylinder walls. Combustion expands the gases and increases swirl to another maximum part way into the power stroke. Expansion of the gases and viscous drag quickly reduce this again before blow-down occurs. But high swirl ratio causes increase in NOx formation therefore, we can reduce it by using proper shaped combustion chamber which can decrease the combustion duration, in other ways we can select the moderate swirl ratio from the result obtained from the simulation as presented in fig5.1. From the result the E50G50 with ethanol temperature 340K have best performance in terms of NOx emission, since the swirl ratio is at average range when compared with the others

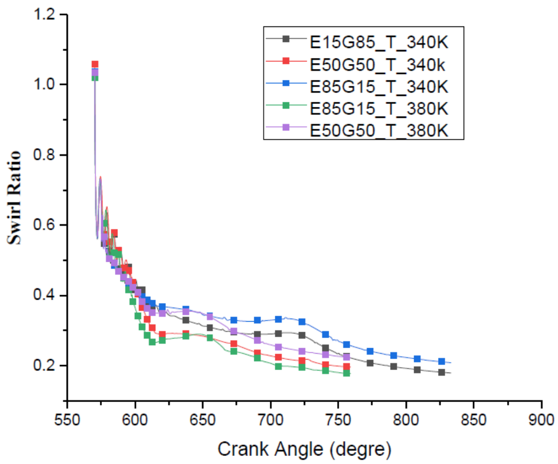


Figure 5.1 swirl ratio for different fuel blend ratio and ethanol temperature

### 5.1.2. Tumble ratio

In order to quantify the turbulence more, a tumble ratio Tca is calculated at each crank angle and plotted in Figure.5.2. The tumble ratio can be interpreted as the ratio of the mean angular velocity of the vortices in the target plane at a certain crank angle which is divided by average crank angle velocity.[29]**.** The negative or positive magnitudes of TR indicate the direction of the overall in-cylinder tumble flow in a given plane as CW or CCW respectively.

The Figure 5.2 shows the variation of the tumble ratio Tca with the crank angle θ. The magnitude of TR maximum when the piston reaches at the mid-plane in between TDC and BDC. The rise in the TR at this point is because of higher piston velocity will occur at this place, in turn which helps tumble motion. When the crank angle θ becomes superior to mid-point and goes to TDC or BDC, the tumble ratio is decreasing and reaching a nil value.

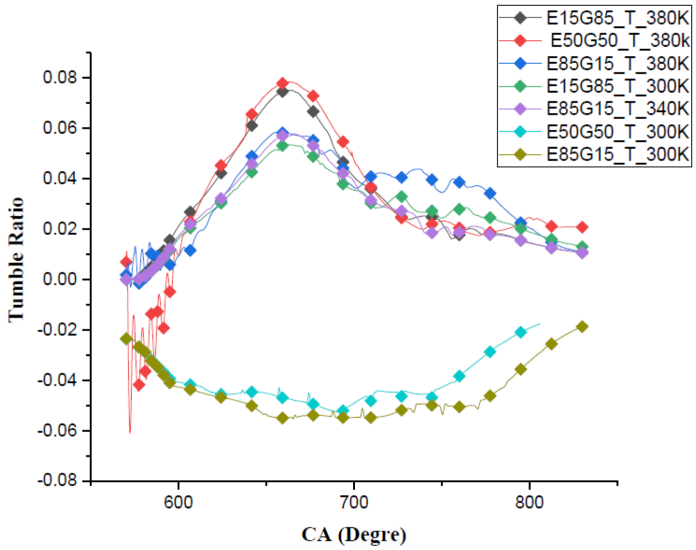


Figure 5.2 variation of Tumble ratio with CA for different ratio and temperature of ethanol fuel

The necessity of tumble motion is to increase the turbulence level which favors proper and quick mixing of fresh charge which leads to effective combustion with reduced emission. The introduction of tumble into the combustion chamber is an effective method of enhancing turbulence intensity prior to ignition, thereby accelerating the burn rates, stabilizing the combustion, and extending the dilution limit. As the engine speed increases (ethanol content or temp increased) flow rate increases with a corresponding increase in swirl, squish and tumble. This increase the rate of fuel evaporation, mixing of fuel vapor and air, and combustion. Air-fuel is consumed within a short time, hence knocking is reduced.

## 5.2. Turbulent Kinetic energy

Fig.5.3 shows the variation of TKE with crank angle for the three fuel ratios of E15G85, E50G50 and E85G15, with different ethanol fuel temperature. From Fig.5.3, in all cases, it is observed that, the TKE varies with crank angle after the fuel injection event. This is because of the transfer of momentum from the injected fuel to the surrounding air. From Fig.5.3, it is also observed that, the rise in TKE is maximum when the ethanol fuel injection temperature is low. At lower fuel injection temperature, the shear deformation of air molecules at the periphery of fuel jet is higher which results in higher fluctuating components of velocity at this region. Therefore, the TKE increases at lower fuel temperatures. Also, the peak TKE after the fuel injection is about 18.9 and 15.41% higher with the fuel injection temperature of 300 and 380 K, compared to that of the 340 K.

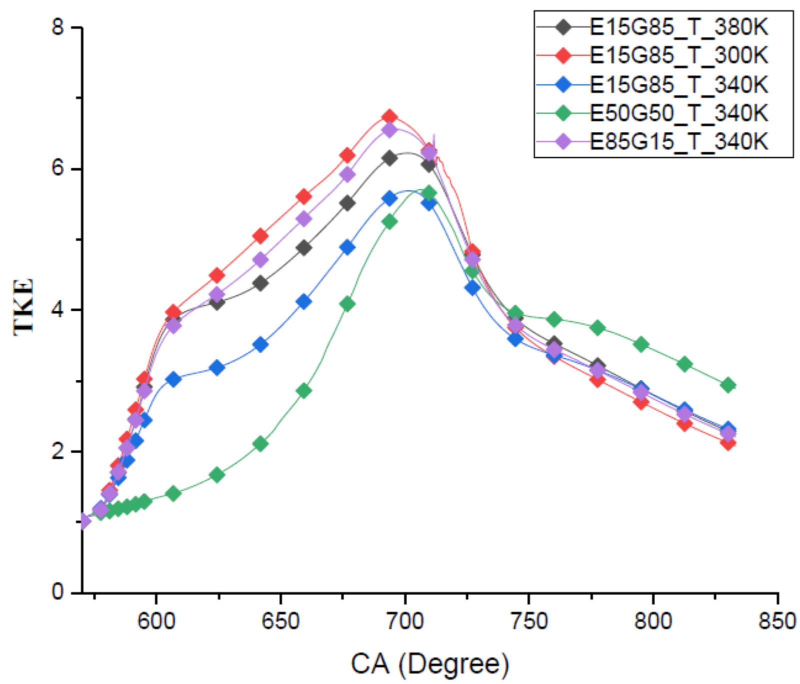


Figure 5.3 Mass-Average Turbulent Kinetic Energy for different percentage and temperature of ethanol fuel

## 5.3. Effect of ethanol ratio and temperature on Cylinder Pressure

In-cylinder pressure is one of most important performance parameters for engine analysis since it measures the combustion characteristics of fuels and engine power [26]**.** pressure is a good parameter to compare engines for design output because it is independent of engine size and/or speed. If torque is used for engine comparison larger engine will always looks better, if power is used as the comparison, speed becomes very important. The pressure field is simulated when the crank angle $\theta$ is ranging from 570° to 833°. The variation of in-cylinder pressure (pressure versus crank angle) at engine speed of 2000 rpm is evaluated for different ethanol temperature and ethanol-gasoline ratios. Figure 5.4 shows the images of contour of pressure captured during the simulation for crank angle varying from 570$^o$ to 833$^o$. The obtained results well represent overall feature of pressure pattern in the cylinder starting from 570 to 833 degrees of crank angle. as we observe from this image the pressure increases during the compression stroke (or for piston moving from BDC to TDC) and it reaches maximum value starting from near to TDC and stay for some degrees and start to decreases for piston moving from TDC to BDC.

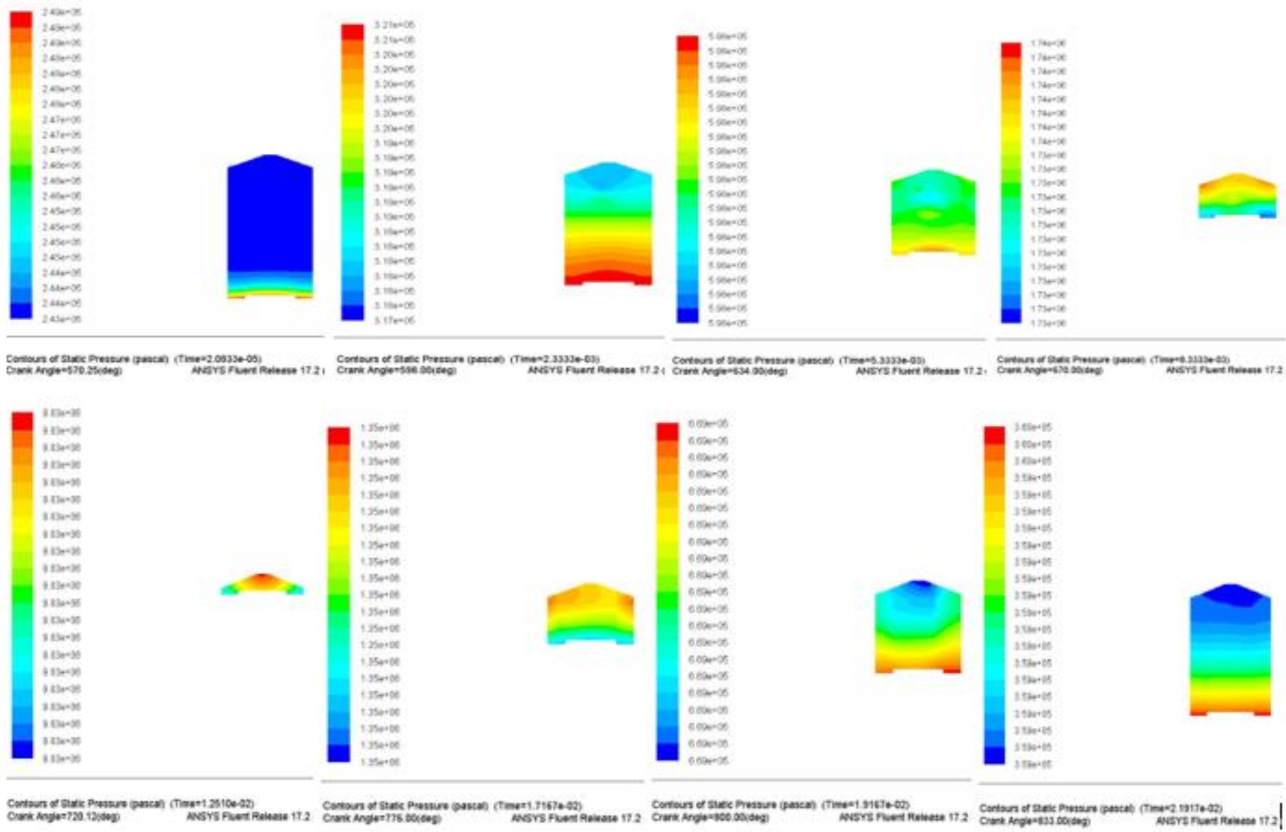

Figure 5.4 Cycle-averaged pressure distribution during the entire simulation for crank angle ranging from 570$^0$ to 833$^0$

Figure 5.5 presents an in-cylinder pressures result of EDI + GPI engine at different temperatures and ratios of ethanol fuel. The variation of in-cylinder pressure is primarily due to the variation in temperature and ratio of ethanol, it can be seen that the maximum pressure for all test fuels occurred closer to top dead center (TDC). In figure 5.5, it is observed that maximum peak in-cylinder pressure is obtained for E50G50 (Ethanol 50% and gasoline 50%) with ethanol inlet temperature of 380K and followed by E50G50 with ethanol temperature of 340K, the peak in-cylinder pressures are about 12 and 10 Mpa, respectively. From figure 5.5, it is observed that, the level of the peak pressure rises by about 15% when the fuel injection temperature increases from 340 to 380 k, which is mainly because of the reduced ignition delay due to better atomization of the fuel at high temperature for this fuel blend (for E50G50 fuel ratio). Also, as observed from a result in fig 5.5, the lowest peak in-cylinder pressure is obtained for E85G15 fuel blend with ethanol fuel temperature of 380K, the peak in-cylinder pressure created inside the combustion chamber is about 7 Mpa. This a reduction in in-cylinder pressure which signifies that enrichment of ethanol fuel with high temperature is incapable of providing sufficient energy density inside the engine cylinder, this is due to the lower energy content of ethanol fuel than gasoline (i.e. ethanol 26.6 KJ/Kg and gasoline 46.6 KJ/Kg) and theoretical air-fuel ratio of gasoline is 1.6 times that of ethanol, therefore, the break specific fuel consumption (BSFC) should be increased with increase of ethanol content. Next to this result, as shown in figure 5.5, the peak in-cylinder pressure decreases noticeably for E15G85 with ethanol fuel temperature 380k. This the reduction of in-cylinder pressure with increase of ethanol fuel ratio and temperature caused by faster combustion speed when ethanol fuel is heated. refereeing to figure 5.5 ethanol fuel with inlet temperature of 340K produce best performance engine for all fuel flex conditions in terms of engine performance and emissions this is because, as depicted in fig. 5.5, the cylinder pressure of the engine is high when operated with ethanol fuel inlet temperature of 340K for all fuel blend ratios.

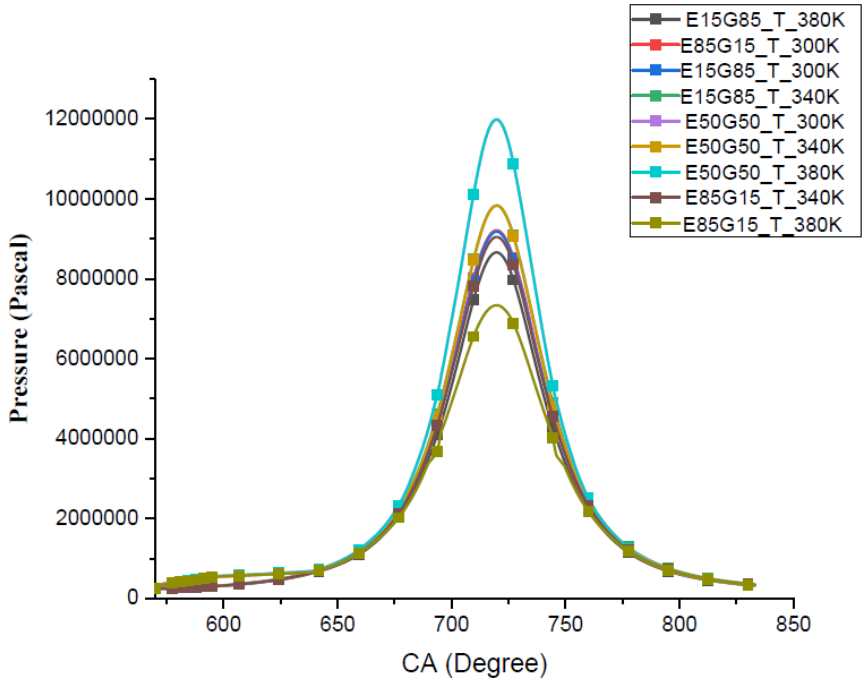


Figure 5.5 Mass-Average Static Pressure for all ratio and temperature of ethanol fuel

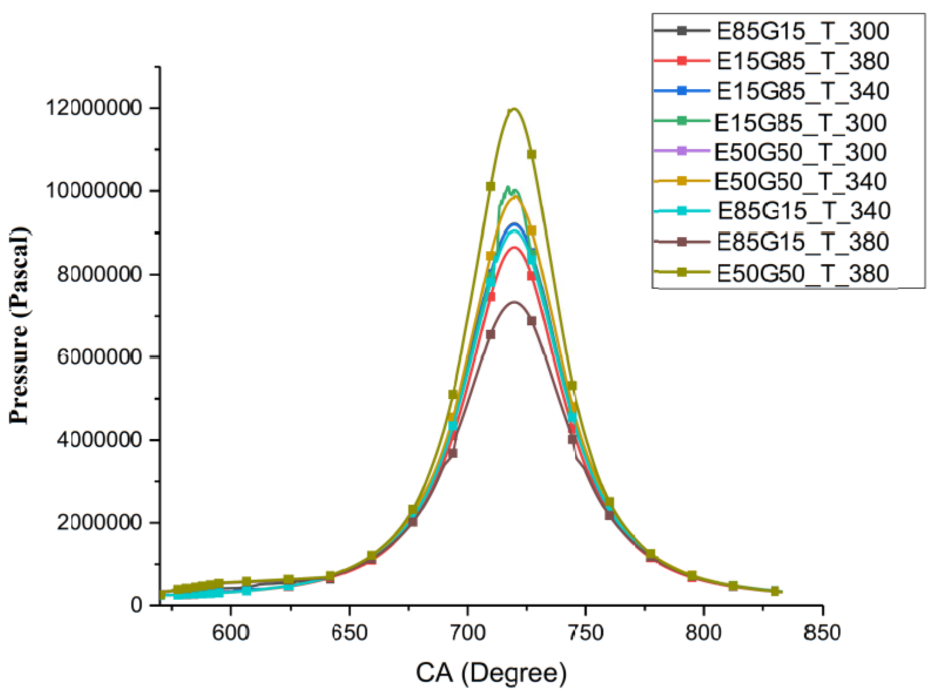


Figure 5.6 Max Static in-cylinder Pressure

## 5.4. Effect of ethanol ratio and temperature on in-cylinder temperatures

The test has been conducted for gasoline port injection and ethanol direct injection engine with pre-heated ethanol fuel at different temperatures like 300 k, 340k and 380k for each ethanol ratio of 15%, 50% and 85% respectively. Figure 5.7 & 5.8 shows the characteristics curves of mass-average and max in-cylinder temperature occurred inside the combustion chamber during compression and power stroke with operation of different ratio and temperature of ethanol fuel. As result shows E15G85 with ethanol temperature of 380K have high in-cylinder temperature and followed by E50G50 with ethanol temperature of 380K. also, E85G15 with ethanol fuel temperature of 380K have high in-cylinder temperature. From this we can observed that when ethanol fuel inlet temperature is increased above 340K the temperature of the combustion chamber increased, this is due to reasons that when ethanol fuel temperature increased further from 340K which is close to ethanol boiling point the ethanol fuel become vapor this leads to the formation of big swirl at the plane of spray or the spray become more turbulent, hence turbulence enhances combustion, also increases the combustion temperature. The second reason, when ethanol fuel temperature increased ethanol fuel loses its charge cooling effect, therefore, the temperature of the combustion chamber increased. This high in-cylinder temperature has its own advantages and disadvantages. The high in-cylinder temperature indicates that the complete combustion occurs inside the combustion chamber this reduce specific fuel consumption of the engine. In other words, it increases fuel efficiency of the engine. And also, reduce the CO and UHC emission of the engine. However, the high temperature has some disadvantages, this high in-cylinder temperature increases the engine heat release rate to the piston and the combustion chamber walls. This means it decreases the thermal efficiency of the engine and it increase the NOx emission of the engine. The lowest in-cylinder temperature is obtained for E50G50 and E15G85 with ethanol temperature of 340K for both fuel blend ratios as shown in fig. 5.7. This the smaller in cylinder temperature have low emission of NOx and heat release rate (heat loss) to the piston and the combustion chamber wall, this means that the thermal efficiency engine is increased with operation of engine with low combustion temperature. However, this smaller in-cylinder temperature causes incomplete combustion of fuels in combustion chamber this increase the emission of carbon-monoxide (CO) and unburned hydro-carbons (UHC). also reduce fuel efficiency of the engine.

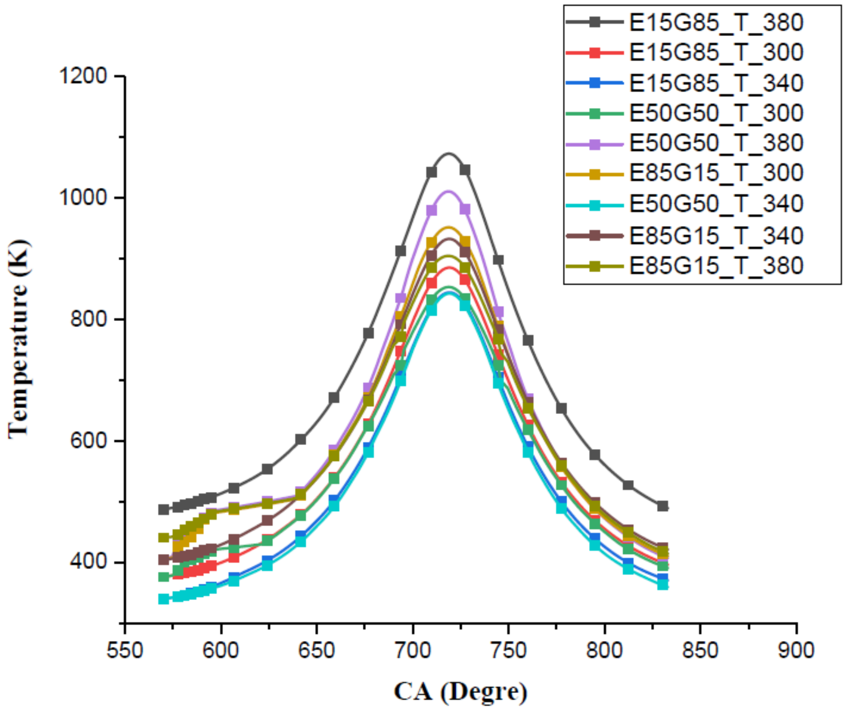


Figure 5.7 Mass-Avg temperature graph for all ethanol-gasoline ratio and temperature

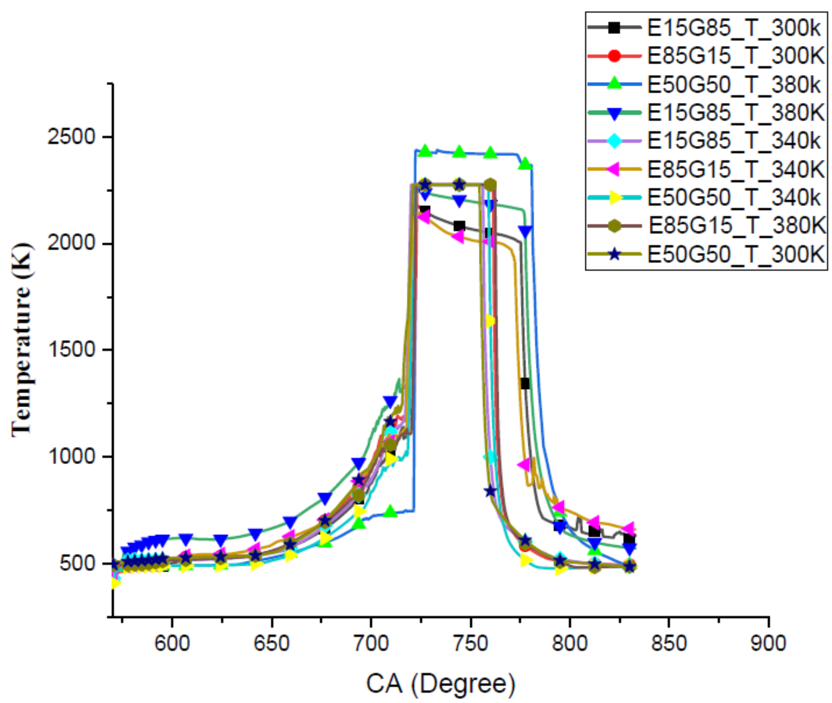


Figure 5.8 Max temperature graph for all ethanol-gasoline ratio and temperature

Figure 5.9 shows the contour of in-cylinder temperature distribution captured for different crank angle. from the figure as the piston moves from 570$^o$ to 720$^o$ (piston moving from BDC to TDC) the temperature of combustion chamber increased and the temperature shoot a maximum value when the spark is ignited and the temperature slightly reduced during the expansion phase.

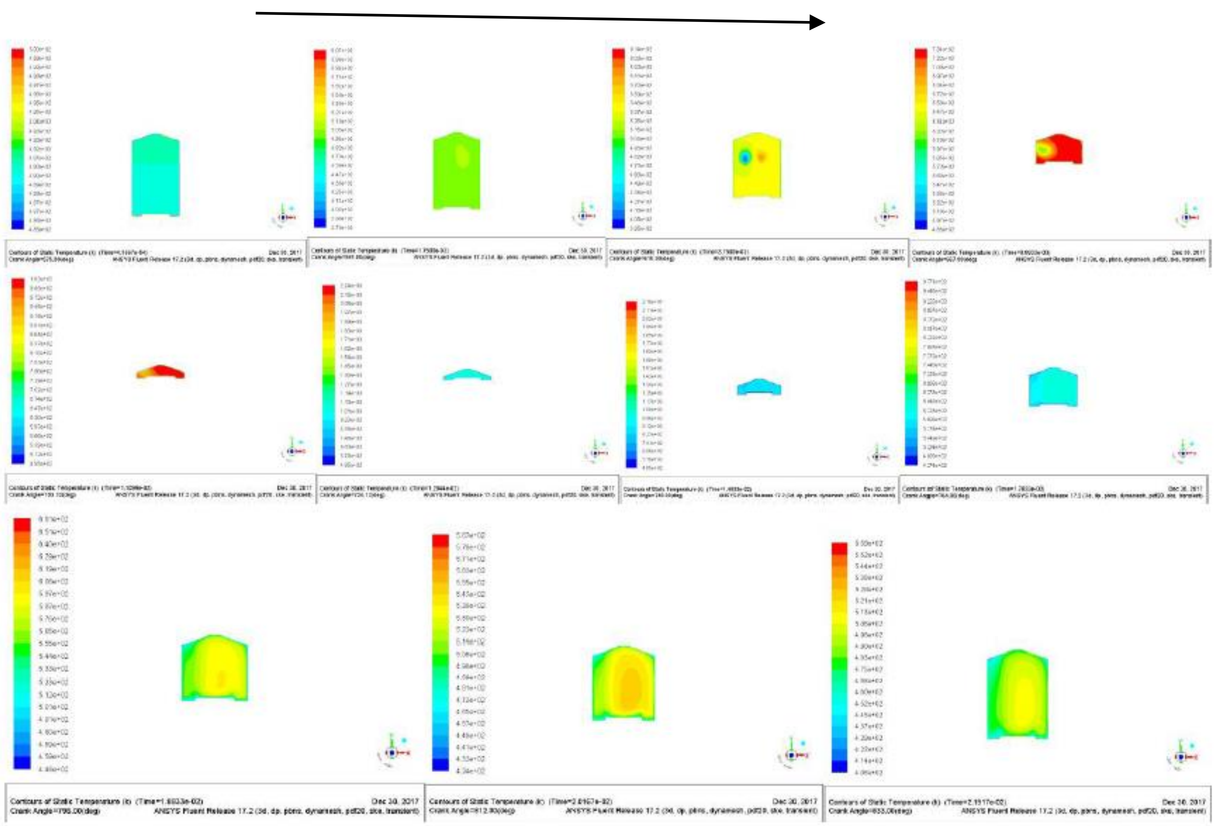

Figure 5.9 contour of temperature distribution inside combustion chamber

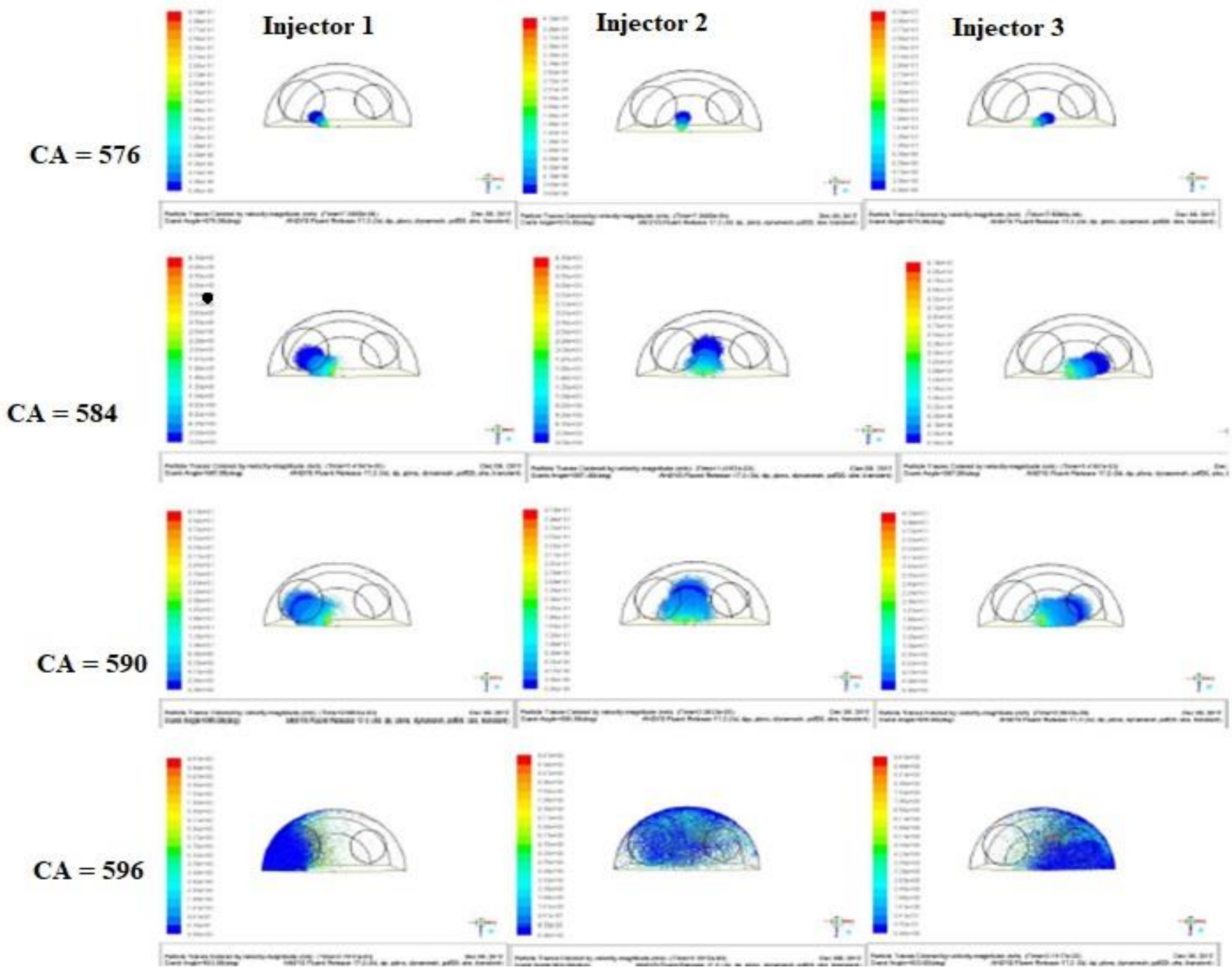


Figure 5.10 velocity distribution of during injection for the three injectors on horizontal plane

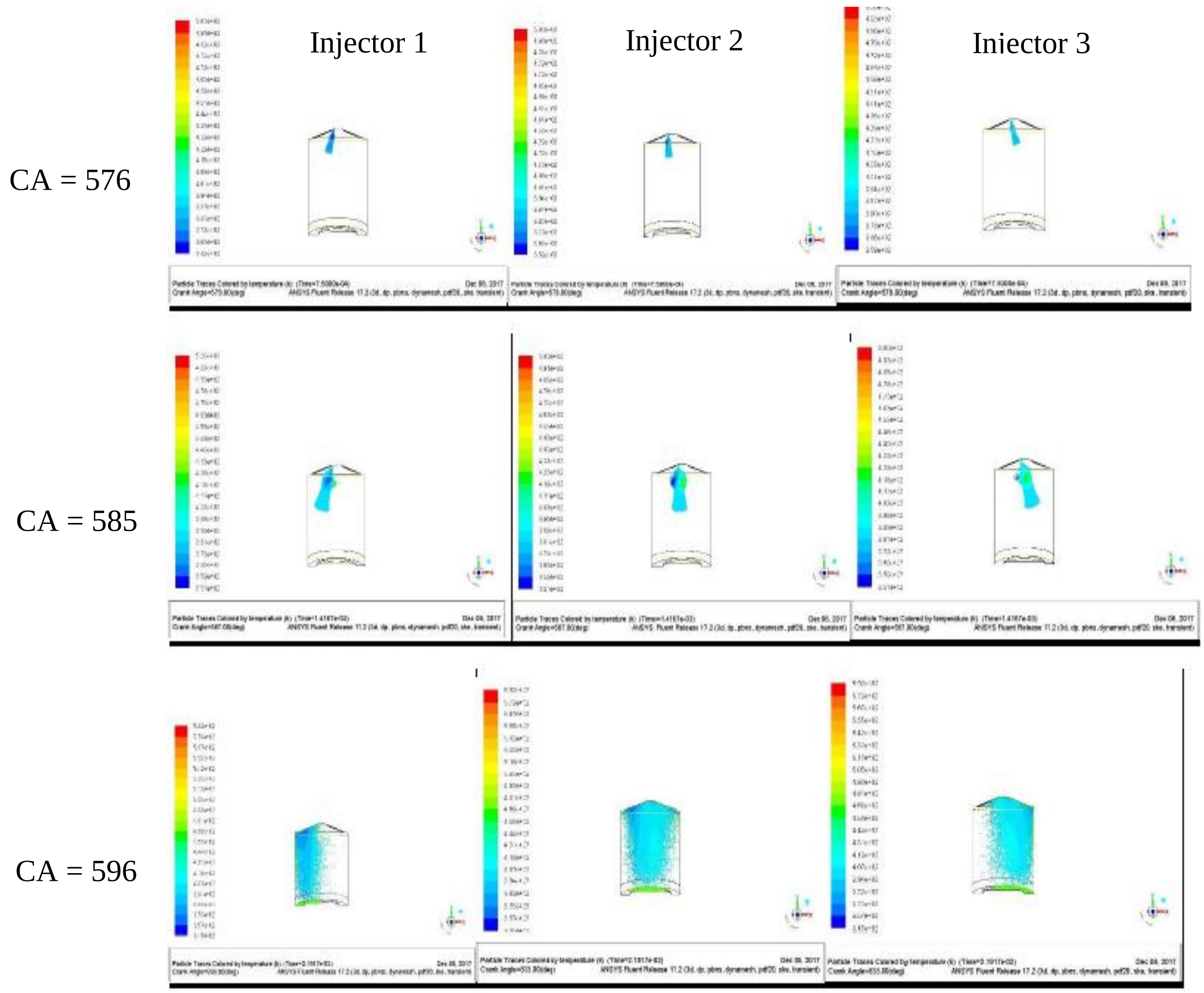


Figure 5.11 Injection temperature for the three injector angles on symetry plane

Figure 5.10 and 5.11 represents images captured by ANSYS software to show the counter of velocity and temperature distribution of ethanol direct injection. The velocity distribution images were captured on horizontal plane at different crank angle and shows the distribution of ethanol fuel inside the combustion chamber during injection (EDI). Fig 5.11 shows the temperature distribution of EDI during the injection period.

## 5.5. Combined analysis of in-cylinder pressure and temperature on engine performance and emission

The effects of ethanol fuel ratio and inlet temperature on SI engine performance was studied in this paper, and the result obtained from the simulation are presented in previous section. These results can be discussed in this section

Fig. 5.5 & 5.7 shows the simulation result of in-cylinder pressure and in-cylinder temperature with crank angle degrees at ethanol ratios from 15% to 85% and ethanol inlet temperature ranging from 300k to 380k. As shown in Fig. 5.5, the peak cylinder pressure increases with the increase of ethanol ratio from 15% to 50% and decreases when the ethanol ratio is further increased from 50% to 85% for all inlet temperature of ethanol fuel. by comparing the result obtained for ethanol blend fuel and pure gasoline fuel the maximum in-cylinder pressure is increased by 22.2% for ethanol fuel ratio of 50% with a temperature of 380K and 0.29% and 0.23% for E15G85 with ethanol temperature of 340k and for E50G50 with ethanol temperature of 340K respectively. From results depicted that, operating the engine with ethanol fuel temperature of 340k produce best engine performance in terms of in-cylinder pressure for all fuel ratios, also, fuel ratio of 50% (i.e. ethanol 50% and gasoline 50%) gives best engine performance.

And from fig. 5.7, it is observed that the in-cylinder temperature decreases when heating ethanol fuel from 300K – 340K for all ratios of ethanol fuel. The maximum reduction of in-cylinder pressure is 5.91% at ethanol ratio of 50% and 5.69% at ethanol ratio of 15% with temperature of 340k for both. It is observed in figure 5.7, that increasing ethanol fuel temperature above 340 K will increase in-cylinder temperature of the combustion chamber. The maximum in-cylinder temperature was increased by 19.76% and 12.79% for E15 and E50 with a temperature of 380K respectively. This is due to reasons that when ethanol fuel temperature increased further from 340K which is close to ethanol boiling point the ethanol fuel become vapor this leads to the formation of big swirl at the plane of spray or the spray become more turbulent, hence turbulence enhances combustion, also increases the combustion temperature. However, when we observe figure. 5.5, the in-cylinder pressure gained by these fuel ratio and temperature is not satisfactory. The maximum in-cylinder temperature in the combustion chamber means the higher heat release rate, NOx emission and the lower in-cylinder pressure, in other words the lower thermal efficiency of the engine. Hence, operating the engine with ethanol 50% and temperature of 340k will increase in-cylinder pressure by 0.23% and reduce in-cylinder temperature by 5.91%. this the reduction of in-cylinder temperature and the accession of in-cylinder pressure will increase the thermal efficiency of the engine. In other words, operating an engine with low in-cylinder temperature will reduce the NOx emission of the engine.

## 5.6. Ethanol fuel pre-heating mechanism

In this section the mechanism of ethanol fuel pre-heating by using the waste heat from engine will be presented. This can be done by constructing counter flow double pipe heat exchanger on the exhaust manifold of the engine, which recover the waste heat released from the exhaust gas of the engine. The simulation for heat exchanger including CAD modelling can be done by using the following parameters, dimensions and incorporating them into engine heat sink designs and selections to find solutions suitable for the maximum heat transfer. The design specification and dimension of heat exchanger selected for EDI heating is presented in table 5.1

Table 5.1 heat exchanger dimension and specifications

| Features | Inner diameter | Outer diameter | length | material |
|---|---|---|---|---|
| Outer tube | 50 mm | 58 mm | 1000 mm | steel |
| Inner tube | 25 mm | 33 mm | 1000 mm | Aluminum |

The 3D CAD model features of heat exchanger which modeled by ANSYS Designmodeler is presented in figure 5.12 with direction of hot and cold fluids.

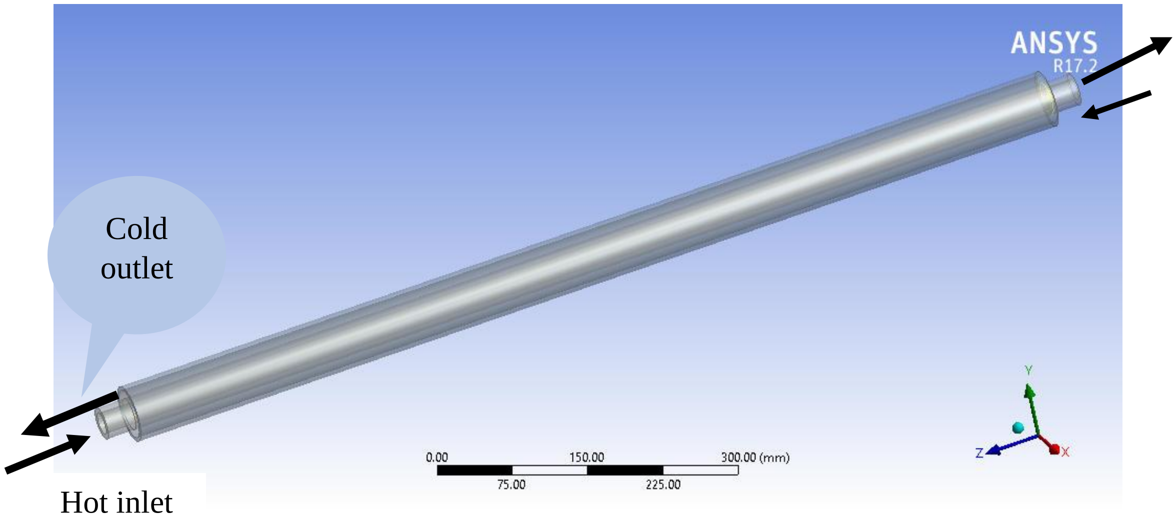


Figure 5.12**; -** 3D CAD model of counter flow double pipe heat exchanger

Since the heat exchanger is designed to recover the heat released from the combustion chamber as exhaust gas from the engine to pre-heat the ethanol fuel before injected to the combustion chamber. Therefore, the engine exhaust temperature and the mass flow rate of ethanol fuel which injected to the combustion chamber is used as the boundary condition for the simulation. i.e. the exhaust temperature of the engine 500K and mass flow rate of ethanol 0.002214 kg/s (result obtained from engine simulation). The result from the simulation of heat exchanger which performed by the above specification and boundary conditions presented in fig.5.13. From figure 5.13 this paper concludes that using counter flow double pipe heat exchanger which exchange heat with exhaust gas from the engine with length of 1m will heat the ethanol fuel up to 390 K and have low pressure drop. hence, by using one-meter heat exchanger on exhaust manifold we can achieve the required ethanol pre-heating temperature and pressure drop of the heat exchanger.

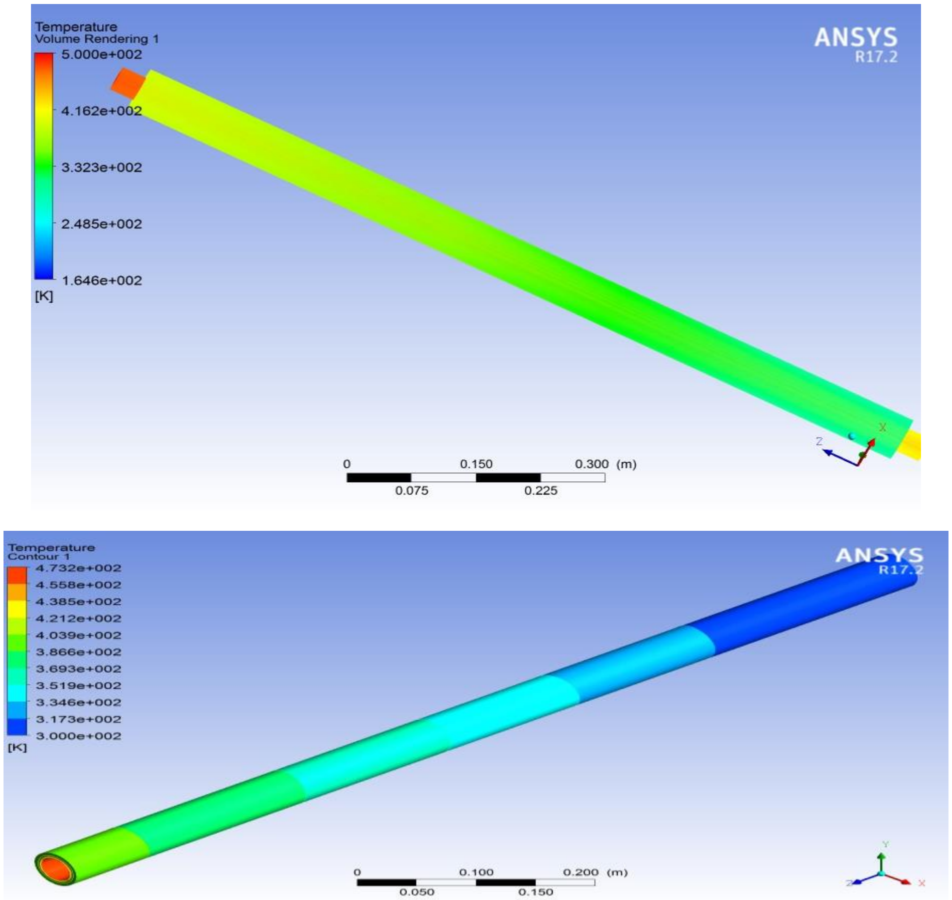


Figure 5.13 Temperature distribution through the heat exchanger

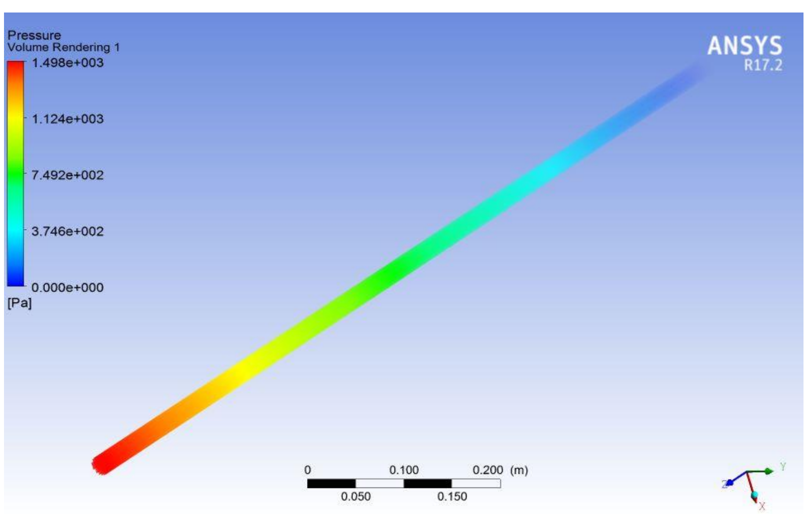


Figure 5.14 contour of pressure through the heat exchanger

# Conclusion

The effects of ethanol fuel ratio and temperature on the engine performance and emission characteristics of a four-stroke EDI + GPI engine is analyzed by using CFD simulation. A comprehensive literature review of EDI + GDI engines has been provided and engine geometry is modeled including necessary data analysis has been applied which enables to simulate SI engine performance and emissions characteristics fueled by ethanol and gasoline. Then simulation results were validated against the experimental data available in the literature. Finally, a detailed analysis was carried out for each ethanol fuel ratio and temperature to predicted performance and emissions characteristics of the engine. From the results, the following conclusions are drawn:

- Increasing ethanol fuel temperature will enhance the formation of turbulence inside the combustion chamber which increases the rate of fuel evaporation, mixing of the fuel vapor and air, and combustion. Hence, the highest turbulence was obtained for higher EDI temperature (i.e. for EDI temperature of 380K) for all fuel blend ratios.
- The peak in-cylinder pressure insignificantly increases with the increase of EDI ratio and temperature from 15% to 50% and 300 to 340K, respectively. And decreases when the ethanol fuel ratio and temperature is further increased from 50% to 85% and 340 to 380K respectively. when ethanol fuel ratio increased from 50% to 85% and temperature increased from 340K to 380K, in-cylinder pressure reduced by 25.1%, due to lower energy density of ethanol fuel and high heat release rate of the engine.
- When increasing the ratio and temperature of ethanol fuel from 15% to 50% and 300K to 340K, respectively, reduces the in-cylinder temperature created inside the combustion chamber during combustion reaction. The maximum reduction of in-cylinder temperature was 5.91% and 5.69% for ethanol ratio of 50% and 15% respectively, with ethanol fuel temperature of 340K.further increasing ethanol temperature from 340K to 380K, increase the in-cylinder temperature of the engine which enhances heat loss and the emission of NOx, in turn reduces in-cylinder pressure and thermal efficiency of the engine. The maximum in-cylinder temperature obtained was 19.76% and 12.79% higher for ethanol ratio of 15% and 50% with ethanol temperature of 380 K for both ratios.
- Finally, the E50% ratio with ethanol inlet temperature of 340k gives lower in-cylinder temperature with higher in-cylinder pressure as compared to those of other blend ratio and

temperature. It gives about 5.91% lower in-cylinder temperature and 0.23% higher in-cylinder pressure as compared to that of pure gasoline. This increase the performance of engine and reduce engine NOx emissions.

- Using counter flow double pipe heat exchanger which exchange heat with exhaust gas from the engine with length of 1m will heat the ethanol fuel up to 390 K with low pressure drop.

# Recommendation

Below are a few suggestions for possible future work that are based on the discoveries and conclusions found during the course of this thesis.

- In future, if the study is done in terms of engine body design and modification for selection of materials and for material handling design.
- It would be interesting if full engine model under full cycle simulation condition were carried out to get relevant output of the engine, which perform a complete cycle simulation during one power cycle.
- It is interesting if experimental work is done to validate and improve the applicability of results obtained on during the investigations.
- The current model does not have independent correlation to predict the formation of NOx, CO and other pollutant emission inside the combustion chamber, it interprets them in terms of in-cylinder pressure and temperature. Therefore, it is interesting if the correlation for these emission parameters was developed which improve the capability of the model to predict the emission from the engine.
- To pre-heat ethanol fuel, if compact type heat exchanger are designed which reduce the length of heat exchanger with optimized efficiency.

# Reference

[1] Y. A. A. J. G. CENGEL, *H E A T A N D M A S S T R A N S F E R*, FIFTH EDIT. New York,: McGraw-Hill Education, 2 Penn Plaza.

[2] “ANSYS Fluent Theory Guide,” vol. 15317, no. August, pp. 724–746, 2016.

[3] P. Systems, “Delphi Multec ® GDi Multi-Hole Fuel Injectors,” pp. 1–2.

[4] S. Gundmalm, “CFD modeling of a four stroke S . I . engine for motorcycle application,” 2009.

[5] W. W. Pulkrabek, “Engineering Fundamentals of the Internal Combustion Engine .”

[6] J. I. M. Kerr, T. Speaking, P. October, G. Motors, and C. Malibu, “Direct vs. port injection,” 2013.

[7] H. Xu, C. Wang, X. Ma, A. K. Sarangi, A. Weall, and J. Krueger-venus, “Fuel injector deposits in direct-injection spark-ignition engines,” *Prog. Energy Combust. Sci.*, vol. 50, pp. 63–80, 2015.

[8] R. Rotondi and G. Bella, “Gasoline direct injection spray simulation ☆,” vol. 45, pp. 168–179, 2006.

[9] N. Jeuland, X. Montagne, and X. Gautrot, “Potentiality of Ethanol as a Fuel for Dedicated Engine *,” vol. 59, no. 6, pp. 559–570, 2004.

[10] N. Kim, S. Cho, and K. Min, “A study on the combustion and emission characteristics of an SI engine under full load conditions with ethanol port injection and gasoline direct injection,” *FUEL*, vol. 158, no. 2015, pp. 725–732, 2017.

[11] Y. Huang, G. Hong, and R. Huang, “Numerical investigation to the dual-fuel spray combustion process in an ethanol direct injection plus gasoline port injection ( EDI + GPI ) engine,” *Energy Convers. Manag.*, vol. 92, pp. 275–286, 2015.

[12] Y. Zhuang, G. Hong, and J. Wang, “Preliminary investigation to combustion in a SI engine with direct ethanol injection and port gasoline injection ( EDI + GPI ),” no.

December, pp. 3–6, 2012.

[13] Y. Zhuang, J. Wang, and G. Hong, "A single cylinder research engine for investigating combustion of direct ethanol injection and port gasoline injection," no. December, pp. 5–8, 2012.

[14] "Ethanol and automobile engines," pp. 1979–1980, 1985.

[15] Y. Huang, G. Hong, and R. Huang, "Investigation to charge cooling effect and combustion characteristics of ethanol direct injection in a gasoline port injection engine," *Appl. Energy*, vol. 160, pp. 244–254, 2015.

[16] Y. Huang, G. Hong, and R. Huang, "Effect of injection timing on mixture formation and combustion in an ethanol direct injection plus gasoline port injection ( EDI þ GPI ) engine," *Energy*, vol. 111, pp. 92–103, 2016.

[17] Y. Huang and G. Hong, "Investigation of the effect of heated ethanol fuel on combustion and emissions of an ethanol direct injection plus gasoline port injection ( EDI + GPI ) engine," *Energy Convers. Manag.*, vol. 123, pp. 338–347, 2016.

[18] Y. Huang, S. Huang, R. Huang, and G. Hong, "Spray and evaporation characteristics of ethanol and gasoline direct injection in non-evaporating , transition and flash-boiling conditions," *ENERGY Convers. Manag.*, vol. 108, pp. 68–77, 2016.

[19] B. Harshavardhan and J. M. Mallikarjuna, "Effect of piston shape on in-cylinder flows and air-fuel interaction in a direct injection spark ignition engine - A CFD analysis," *Energy*, vol. 81, no. January, pp. 361–372, 2015.

[20] T. I. No, "All About Spark Plugs," *Beru*, no. 2.

[21] D. F. Injection and D. T. Guide, "1 . 1 Purpose of Fuel Injection System," pp. 1–6, 2013.

[22] D. P. D. THEODORE L. BERGMAN, ADRIENNE S. LAVINE, FRANK P. INCROPERA, *Fundamentals of Heat and Mass Transfer*, SEVENTH ED. .

[23] F. Joshua, "Design and Construction of a Concentric Tube Heat Exchanger," vol. 13, no. 2, pp. 128–133, 2009.

[24] Ansys, “Internal Combustion Engines in Workbench,” vol. 15317, no. November, pp. 1–542, 2013.

[25] A. D. Canonsburg, “Internal Combustion Engines in Workbench,” vol. 15317, no. April, pp. 724–746, 2015.

[26] A. M. Pourkhesalian, A. H. Shamekhi, and F. Salimi, “Alternative fuel and gasoline in an SI engine : A comparative study of performance and emissions characteristics,” *Fuel*, vol. 89, no. 5, pp. 1056–1063, 2010.

[27] L. Liang, R. D. Reitz, J. Yi, and C. O. Iyer, “A G -equation Combustion Model Incorporating Detailed Chemical Kinetics for PFI / DI SI Engine Simulations G -equation description of turbulent,” 2006.

[28] B. H. Pitsch, “A G -equation formulation for large-eddy simulation of premixed turbulent combustion,” 2002.

[29] Z. Barbouchi and J. Bessrour, “Turbulence study in the internal combustion engine,” vol. 1, no. 9, pp. 194–202, 2009.